Molecular Plant
Research Article

CellPress
PARTNER JOURNAL

Functional Accumulation of Antenna Proteins in Chlorophyll *b*-Less Mutants of *Chlamydomonas reinhardtii*

Sandrine Bujaldon[1,5], Natsumi Kodama[2,3,5], Fabrice Rappaport[1,6], Rajagopal Subramanyam[4], Catherine de Vitry[1], Yuichiro Takahashi[2,3,*] and Francis-André Wollman[1,*]

[1]Institut de Biologie Physico-Chimique, UMR7141 CNRS-UPMC, Paris 75005, France

[2]Research Institute for Interdisciplinary Science, Okayama University, Okayama 700-8530, Japan

[3]JST-CREST, Okayama University, Okayama 700-8530, Japan

[4]Department of Plant Sciences, School of Life Sciences, University of Hyderabad, Hyderabad 500046, India

[5]These authors contributed equally to this article.

[6]Deceased while manuscript was in progress.

***Correspondence: Yuichiro Takahashi (taka@cc.okayama-u.ac.jp), Francis-André Wollman (wollman@ibpc.fr)**

http://dx.doi.org/10.1016/j.molp.2016.10.001

ABSTRACT

The green alga *Chlamydomonas reinhardtii* contains several light-harvesting chlorophyll *a*/*b* complexes (LHC): four major LHCIIs, two minor LHCIIs, and nine LHCIs. We characterized three chlorophyll *b*-less mutants to assess the effect of chlorophyll *b* deficiency on the function, assembly, and stability of these chlorophyll *a*/*b* binding proteins. We identified point mutations in two mutants that inactivate the *CAO* gene responsible for chlorophyll *a* to chlorophyll *b* conversion. All LHCIIs accumulated to wild-type levels in a *CAO* mutant but their light-harvesting function for photosystem II was impaired. In contrast, most LHCIs accumulated to wild-type levels in the mutant and their light-harvesting capability for photosystem I remained unaltered. Unexpectedly, LHCI accumulation and the photosystem I functional antenna size increased in the mutant compared with in the wild type when grown in dim light. When the *CAO* mutation was placed in a yellow-in-the-dark background (yid-BF3), in which chlorophyll *a* synthesis remains limited in dim light, accumulation of the major LHCIIs and of most LHCIs was markedly reduced, indicating that sustained synthesis of chlorophyll *a* is required to preserve the proteolytic resistance of antenna proteins. Indeed, after crossing yid-BF3 with a mutant defective for the thylakoid FtsH protease activity, yid-BF3-*ftsh1* restored wild-type levels of LHCI, which defines LHCI as a new substrate for the FtsH protease.

Key words: *Chlamydomonas reinhardtii*, chlorophyll *b*-less mutant, antenna protein, *CAO* gene

Bujaldon S., Kodama N., Rappaport F., Subramanyam R., de Vitry C., Takahashi Y., and Wollman F.-A. (2017). Functional Accumulation of Antenna Proteins in Chlorophyll *b*-Less Mutants of *Chlamydomonas reinhardtii*. Mol. Plant. **10**, 115–130.

INTRODUCTION

In oxygenic photosynthesis, photosynthetic electron flow is driven by photochemical reactions in two photosystems that use light energy captured by antenna pigments. In the green lineage, these light-harvesting pigments are found in core antennae and peripheral antennae complexes. The core antenna is made exclusively of chlorophyll *a* (Chl *a*), either bound to CP43 and CP47 encoded by the chloroplast *psbC* and *psbB* genes, next to the reaction center of photosystem II (PSII), or within the reaction center of photosystem I (PSI), consisting of the PsaA/PsaB heterodimer, encoded by the chloroplast *psaA* and *psaB* genes. The peripheral antenna complexes, which bind both Chl *a* and chlorophyll *b* (Chl *b*), are designated light-harvesting Chl *a*/*b* complexes. Those complexes that transfer excitons to photosystems I or II (PSI or PSII) reaction centers are designated as light-harvesting complexes I and II (LHCI and LHCII), respectively. Besides several types of major LHCIIs there are three minor LHCII complexes in plant chloroplast, CP24, CP26, and CP29. The crystal structures of the major LHCII, minor LHCII (CP29), and LHCI in PSI–LHCI supercomplexes revealed that not only the amino acid sequence but also the three-dimensional structure

Published by the Molecular Plant Shanghai Editorial Office in association with Cell Press, an imprint of Elsevier Inc., on behalf of CSPB and IPPE, SIBS, CAS.

is well conserved among different LHCs; these exhibit three transmembrane helices (helices A, B, and C) and two short amphipathic helices (helices D and E).

Chl *b*, which is produced from Chl *a* by the action of the chlorophyll oxygenase encoded by the *CAO* gene (Tanaka et al., 1998; Espineda et al., 1999) is, together with Chl *a*, the major light-harvesting pigment present in the green lineage. When present in a chlorophyll-binding protein, it is diagnostic of it being part of a peripheral light-harvesting antenna, although the Chl *a*/Chl *b* ratios differ widely with the type of light-harvesting complex. The major LHCII from spinach contains eight Chl *a* and six Chl *b* molecules (Chl *a*/Chl *b* ratio of 1.3) as well as two lutein, one neoxanthin, and one carotenoid involved in the xanthophyll cycle (Liu et al., 2004). The minor LHCII from spinach, CP29, contains eight Chl *a*, four Chl *b*, and one possible mixed site for Chl *a* and Chl *b* as well as one molecule of lutein, violaxanthin, and neoxanthin (Pan et al., 2011). In contrast, the pigment content of LHCI is rather variable; Lhca1, Lhca2, Lhca3, and Lhca4 of a plant PSI–LHCI supercomplex contain 12 Chl *a*/2 Chl *b*, 9 Chl *a*/5 Chl *b*, 13 Chl *a*/1 Chl *b*, and 11 Chl *a*/4 Chl *b* molecules, respectively (Mazor et al., 2015; Qin et al., 2015).

The organization of the peripheral antenna in the unicellular alga *Chlamydomonas reinhardtii* is similar to that in vascular plants but displays some characteristic features. In *Chlamydomonas*, the major LHCII proteins are encoded by nine genes (*LHCBM1–9*) and are grouped into four types, types I–IV. LHCII type I is encoded by *LHCBM3*, *4*, *6*, *8*, and *9*; LHCII type II by *LHCBM5*; LHCII type III by *LHCBM2* and *7*; and LHCII type IV by *LHCBM1* (Minagawa and Takahashi, 2004; Natali et al., 2014). *Chlamydomonas* has two minor LHCII proteins, CP26 and CP29, but lacks CP24 (Minagawa and Takahashi, 2004). *Chlamydomonas* also contains nine major LHCI proteins (Lhca1–9) that are stably associated with PSI core complex in PSI–LHCI supercomplex (Takahashi et al., 2004), all of which appear to accumulate to nearly stoichiometric amount (Drop et al., 2011). Here again the antenna composition is different from that in vascular plants, since the latter display only four major LHCI proteins (Lhca1–4) stably associated with the PSI core complex to form PSI–LHCI supercomplexes (Mazor et al., 2015; Qin et al., 2015) and two minor LHCI proteins (Lhca5 and Lhca6), which are present in PSI–NDH supercomplexes (Peng et al., 2009).

Originally, mutants lacking in Chl *b* from vascular plants (Markwell et al., 1985; Terao et al., 1985; Murray and Kohorn, 1991; Takabayashi et al., 2011) or unicellular algae (Michel et al., 1983; Picaud and Dubertret, 1986; de Vitry and Wollman, 1988; Allen and Staehelin, 1994; Polle et al., 2000) were instrumental for a better understanding of the light-harvesting processes in oxygenic photosynthesis, leading to the view that the numerous apoproteins of Chl *a*/*b* complexes have contrasting abilities to withstand the absence of Chl *b*, with LHCI being less Chl *b*-sensitive than LHCII. Later, it was recognized that peripheral antennae not only have a light-harvesting function but also contribute to photoprotection (for a review see Dall'Osto et al., 2015). The latter function explains why several mutants with compromised peripheral antennae display a decreased ability to cope with excess light, thus leading to an increased photosensitivity that is damaging to thylakoid membrane proteins (Elrad et al., 2002) (but see Ferrante et al., 2012 for another situation). Thus, we wished to revisit the phenotype of Chl *b*-less mutants in *Chlamydomonas* in dim versus moderate light intensity, since we aimed at a characterization of the mutant phenotype under conditions that minimized the possible deleterious effect of light on the light-harvesting antennae when Chl *b* is absent.

About three decades ago, several mutants of *Chlamydomonas* lacking Chl *b* had been biochemically characterized to some extent without the molecular identification of their genetic lesion (Picaud and Dubertret, 1986; de Vitry and Wollman, 1988). More recently, another series of genetically well-characterized deletion mutants from *Chlamydomonas* that lacked Chl *b* led to the identification of the *CAO* gene responsible for Chl *a* to Chl *b* conversion (Tanaka et al., 1998). However, none of these mutants displayed a genetic defect restricted to the *CAO* gene, therefore raising the possibility that part of the mutant phenotypes would arise from other changes than those due to the lack of CAO activity per se. Here we compared a *CAO*-encompassing deletion mutant with two other Chl *b*-less mutants, whose genetic lesions were not known, and showed that these are allelic. We then explored in more depth, at two light intensities for growth, the phenotype of the BF3 mutant, which harbors a point mutation in the *CAO* gene, thus providing a robust description of some unexpected light-harvesting changes arising from a specific lesion in the *CAO* gene in *Chlamydomonas*.

RESULTS

Genetic Characterization of Chl *b*-Less Mutants

cbs3 is a Chl *b*-less mutant that harbors a large DNA deletion that compromises expression of eight nuclear genes including the chlorophyll *a* oxygenase (*CAO*) gene responsible for Chl *b* formation (Tanaka et al., 1998). Two other UV-generated mutants, BF3 and *pg27*, have been described earlier as devoid of Chl *b* (Picaud and Dubertret, 1986; de Vitry and Wollman, 1988), but their nuclear mutations had not yet been characterized. The three mutants indeed displayed a total absence of Chl *b*, as shown by chromatography (Figure 1A), and they had a low-fluorescence phenotype when grown in moderate light (Figure 1B). We first wished to know whether the lack of Chl *b* in the BF3 and *pg27* mutants originated from mutations in the *CAO* gene or in some other gene controlling Chl *b* accumulation in *Chlamydomonas*. Since the three mutants showed a similar low-fluorescence phenotype, we screened the progeny of BF3 and *pg27* crosses to *cbs3* for restoration of a wild-type fluorescence phenotype. Such a recovery in crosses would occur only if mutations were in different loci, thus allowing recombination that yields both double mutants and wild-type progeny. Not a single wild-type clone was recovered from these crosses, out of 125 progeny for *cbs3*xBF3 and 137 progeny for *cbs3*x*pg27* (results not shown). Since the three mutations were tightly linked, we PCR-amplified the *CAO* genomic DNA sequence from the mutants. We identified a single C to T substitution in BF3 and a CC to TT substitution in *pg27*, both of which generating a TAG stop codon that led to a premature termination of the *CAO* coding sequence after the 32nd and

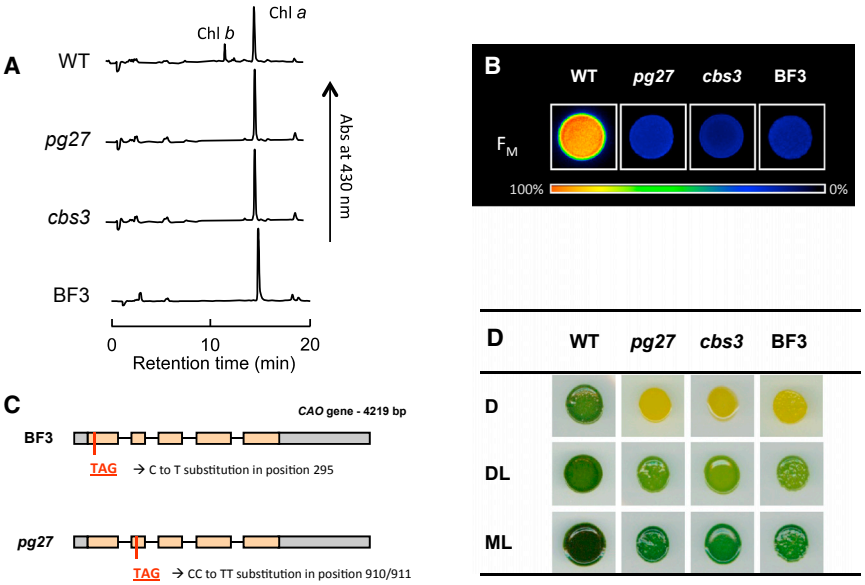

Figure 1. Phenotypes of the Three Chl *b*-Less Mutants.

(A) Detection of Chl *a* and Chl *b* by HPLC. WT, wild-type.

(B) Maximal fluorescence (F_M) of wild-type (WT) and Chl *b*-less mutants grown onto solid TAP medium under moderate light (the color bar represents the fluorescence level).

(C and D) Map of the *CAO* gene in two Chl *b*-less mutants (BF3 and *pg27*) **(C)** and their growth patterns **(D)**. Cultures were spotted on TAP under different light conditions, darkness (D), dim light (DL; 1–2 μmol photons m^{-2} s^{-1}), and moderate light (ML; 50 μmol photons m^{-2} s^{-1}).

165th residue, respectively (Figure 1C). When comparing their growth characteristics under different light regimes, the three mutants showed an unexpected yellow-in-the-dark (yid) phenotype (Figure 1D). To assess whether the yid phenotype was a consequence of the mutations in the *CAO* gene, we backcrossed each mutant to a wild-type strain that had a green-in-the-dark (gid) phenotype. In the three cases, we recovered a gid progeny (Figure 2A) that lacked Chl *b*, as shown by their low-fluorescence phenotype when grown under moderate light intensity (Figure 2B). Complementation of the mutation in gid-BF3 with a wild-type copy of the *CAO* gene resulted in the loss of this low-fluorescence phenotype (Figure 2B) and a restoration of Chl *b* synthesis, as evidenced by an F_V/F_M and a Chl *a*/*b* ratio similar to those in the wild-type (Table 1). Complementation of the mutation in gid-*pg27* with the *CAO* gene gave the same results (data not shown). These data indicate that the three mutants are allelic. In the subsequent experiments, we named *cbs3*, *pg27*, and BF3 the gid versions of the Chl *b*-less mutants but used the prefix yid together with the mutant names when characterizing the yellow-in-the-dark versions of these mutants.

Characterization of the Antenna in Chl *b*-Less Mutants

Table 1 shows the major phenotypic traits of the three *CAO* mutants when grown at two light intensities, using either dim light (~2 μmol photons m^{-2} s^{-1}) or moderate light (50 μmol photons m^{-2} s^{-1}). The various parameters, which are presented in Table 1, show that the three allelic mutants had the same phenotype. They displayed a low-fluorescence phenotype which, under moderate light, could be ascribed in part to a ~30% decrease in chlorophyll content per cell. Still, their maximal fluorescence levels on a cell basis was about 2.5 to 3 times lower than in the wild-type when grown either under a dim light or a moderate light regime. This indicates that the low-fluorescence phenotype of the three Chl *b*-less mutants was largely due to some fluorescence quenching that is not present in the wild-type. Such a change in antenna organization may also be responsible for the much lower F_V/F_M in the mutants, the value of which combines the maximal activity of PSII with the efficiency of the connection between the peripheral antennae and the PSII cores.

Emission spectra were recorded at 77 K for the three mutants grown under dim light or moderate light regimes (Figure 3). In both cases wild-type and mutant cells were vigorously aerated to preserve state 1, i.e., conditions that favor association of the LHCII peripheral antenna with PSII (Nawrocki et al., 2016). In *Chlamydomonas*, the wild-type emission spectrum at 77 K (Figure 3A) is characterized by two major peaks: an emission peak at 685 nm with a shoulder around 695 nm, both of which are emitted by the PSII cores (Wollman and Delepelaire, 1984), and an emission peak in the 713–717 nm region that originates from the PSI cores (Wollman and Bennoun, 1982). The 77 K emission spectra of the Chl *b*-less mutants showed considerable changes with respect to the wild-type spectrum. It was dominated by a major emission peak at 709 nm, with only a small shoulder at 685 nm (Figure 3A). These spectra are reminiscent of those of PSI mutants lacking PSI cores, in which the LHCI antenna emits at 707 nm (Wollman and Bennoun, 1982). This particular feature was retained, independent of the light regime (Figure 3B).

The enhanced emission at 708–709 nm and the low F_V/F_M of the Chl *b*-less mutants suggested that considerable changes had occurred in their light-harvesting properties and/or in their content in PSI and PSII reaction centers. We thus measured the ratio of PSII to PSI reaction centers and the size of their functional antenna. To this end we used the electrochromic shift (ECS) produced by PSI and PSII charge separations after a single-turnover actinic flash in the wild-type and the BF3 mutant. In the wild-type the ECS spectrum in the 460–540 nm region has a typical "S" shape, with minima at 477 nm and maxima at 516 nm, as expected from the absorption shift of several carotenoids, Chl *a*, and Chl *b* (Schmidt et al., 1971; Witt, 1979). Since BF3 is devoid of Chl *b*, its ECS spectrum showed significant changes with respect to the wild-type spectrum (Figure 4A). However, it retained a typical S shape with minima at 492 nm and maxima at 512 nm, as predicted by Witt (1979) for a signal originating only from lutein/Chl *a* complexes. We chose 520 nm as an appropriate wavelength to build the ECS saturation curves from the two strains, after checking that the 520 nm signal responded as a linear probe of the electric field, i.e., that it

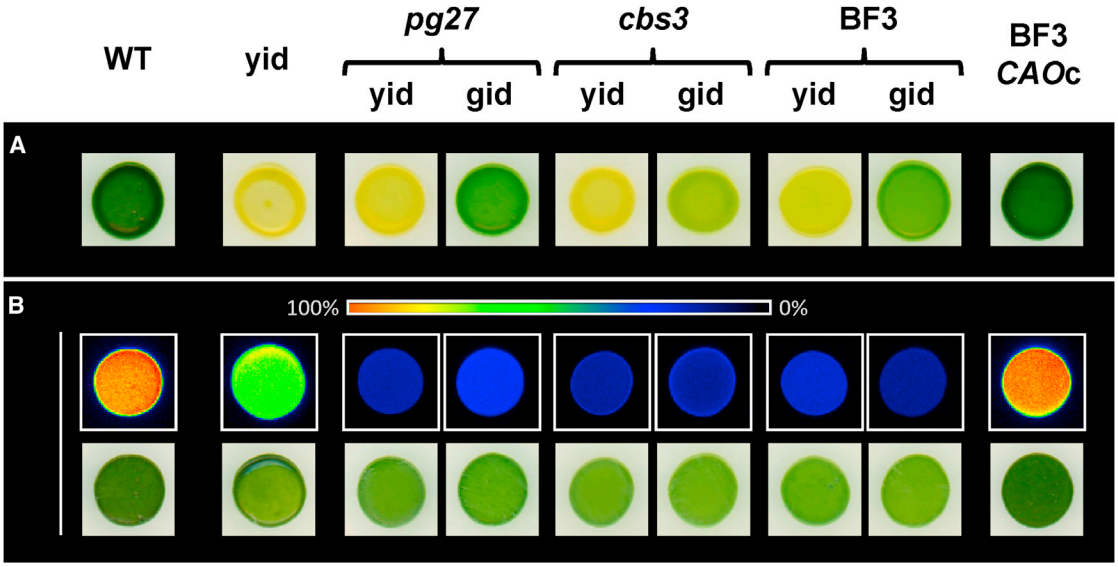

Figure 2. Growth Patterns and Maximal Fluorescence in Green- and Yellow-in-the-Dark Background.
(A and B) Growth patterns of wild-type control (WT), yellow-in-the-dark strain control (yid), Chl *b*-less mutants (*pg27*, *cbs3*, and BF3) yellow-in-the-dark (yid-) and green-in-the-dark (gid-) and the complemented BF3 mutant (BF3-*CAO*c) grown onto solid TAP medium in **(A)** dark and **(B)** under moderate light, and their maximal fluorescence (the color bar represents the fluorescence level).

doubled when two actinic flashes were given in the two strains (experiment not shown). The results from three biological replicates are gathered in Figure 4B and typical experiments allowing the measurement of the PSII and PSI antenna sizes by ECS are presented in Figure 4C, where data points are fitted with only one exponential. We first observed that the ratio of PSII to PSI centers, calculated from the ECS signals obtained using a saturating flash (see Methods), were similar in BF3 and wild-type, with a 20%–30% increase in dim light compared with moderate light (Figure 4B). Therefore, the presence of a major 708 nm emission peak observed in BF3 does not reflect a loss of PSI centers in Chl *b*-less mutants. The new 77 K emission at 709 nm then should originate from some Chl *b*-less peripheral antenna. We measured the relative PSII functional antenna sizes by comparing either the half-time of the fluorescence induction rise in the presence of 3-(3,4)-dichlorophenyl-1,1-dimethylurea (DCMU) or the light-saturation curves for the ECS signal after a single-turnover flash. We observed that, whether it was grown in very dim light or at moderate light intensity, the BF3 mutant displayed a functional PSII antenna size that was about two times smaller than the wild-type (Figure 4B and 4C, left panels). Most unexpectedly, the PSI antenna size in the BF3 mutant was 60% larger than that in the wild-type when cells were grown in dim light (Figure 4B and 4C, right panels). However, it became similar to that in the wild-type when cells were grown at moderate light intensity.

To understand how the changes in functional antenna sizes in the BF3 mutant compared with its actual content in peripheral antenna proteins, we investigated their accumulation level by immunoblotting the whole-cell protein content against specific antibodies to core and antenna subunits of PSII and PSI. As Figure 5A shows, the minor and major peripheral antenna proteins of PSII—CP29, LHCII types I, II (Lhcbm5), III, and IV—accumulated to identical levels, on a chlorophyll basis, in the wild-type and BF3 mutant, independent of the light regime for growth. Only CP26 showed, together with D1, a limited increase in the BF3 mutant when compared with the wild-type on a chlorophyll basis. Thus, when compared with the content in D1 protein, an indicator of the content in PSII cores, the peripheral antenna proteins, except for CP26, showed a limited decrease in the mutant although their stoichiometry relative to one another remained unchanged.

We then analyzed the accumulation of the nine LHCI proteins that make up the PSI peripheral antenna in *Chlamydomonas* (Takahashi et al., 2004). The recognition patterns of the antibodies to each of the nine Lhca subunits are shown in Supplemental Figure 1. Each Lhca subunit can be detected specifically with the appropriate antibody. For an easier comparison with functional measurements, we estimated the accumulation of LHCI proteins on a PSI core basis. Total cell proteins were loaded onto SDS–polyacrylamide gels to deliver the same signal intensity of PSI subunits, and the relative signal intensity of LHCI proteins was compared in the wild-type and BF3 mutant under the two light regimes for growth. As shown in Figure 5B, we detected the signals of the major PSI proteins, PsaA, PsaD, PsaF, PsaK, PsaH, PsaL, and PsaN, at a similar intensity in all cases. Only PsaG showed enhanced accumulation in the BF3 mutant compared with the wild-type under the two light regimes. When the BF3 mutant was grown in moderate light, Lhca4 showed a slight decrease in accumulation, whereas most LHCI subunits accumulated at a level similar to that of the wild-type. In contrast, the accumulation of LHCI subunits was deeply modified when the BF3 mutant was grown in dim light. Six of the LHCI proteins, Lhca1, Lhca3, Lhca5, Lhca7, Lhca8, and Lhca9, showed a marked increase in the BF3 mutant whereas two other LHCI proteins, Lhca4 and Lhca6, showed a decreased accumulation, Lhca2 remaining at a level close to that in the wild-type. Thus,

Parameter		WT	*cbs3*	*pg27*	BF3	BF3-*CAOc*
[Chl] (μg/10^6 cell)	DL	1.2 ± 0.2	1.1 ± 0.2	0.7 ± 0.3	1.05 ± 0.01	1.80 ± 0.07
	ML	2.0 ± 0.3	1.6 ± 0.1	1.3 ± 0.4	1.3 ± 0.3	2.8 ± 0.2
Chl *a*/*b*	DL	2.9 ± 0.2	–	–	–	2.9 ± 0.2
	ML	3.1 ± 0.1	–	–	–	3.5 ± 0.2
F_M/Cell	DL	100%	38% ± 3%	32% ± 6%	35% ± 4%	124% ± 5%
	ML	100%	39% ± 8%	40% ± 4%	36% ± 8%	73% ± 11%
F_V/F_M	DL	0.75 ± 0.02	0.42 ± 0.08	0.30 ± 0.04	0.28 ± 0.09	0.76 ± 0.01
	ML	0.75 ± 0.01	0.49 ± 0.06	0.34 ± 0.03	0.45 ± 0.04	0.63 ± 0.04

Table 1. Chlorophyll and Fluorescence Parameters of Wild-Type Control (WT), Chl *b*-Less Mutants Green-in-the-Dark (*cbs3*, BF3, *pg27*), and the Complemented BF3 Mutant.

Chlorophyll concentrations were determined according to Porra et al. (1989). Percentage was determined by comparison of the mutant with the wild-type cells grown under the same light condition. Values represent means ± SD (n = 3–10). DL, dim light (1–2 μmol photons m^{-2} s^{-1}); ML, moderate light (50 μmol photons m^{-2} s^{-1}).

the absence of Chl *b* caused a deep change in the stoichiometry of the various Lhca proteins within LHCI, which resulted in a net increase in the overall content of LHCI relative to the PSI cores.

Phenotype of Chl *b*-Less Mutants in which Chlorophyll Synthesis Is Limited in Dim Light

We then looked for the peripheral antenna content in the yid version of the *CAO* mutants to assess how the absence of Chl *b* affects the greening process (Figure 6). Indeed yid-*cbs3*, yid-*pg27*, and yid-BF3 displayed a pale-green phenotype when grown in dim light (Figure 1D) and had a lower chlorophyll content per cell when compared with their gid counterpart (see Table 2 versus Table 1), which suggests additional antenna defects. When immunoblots of whole-cell protein extracts were performed with the yid-BF3 grown under moderate light, we observed the same LHCI and LHCII profiles as in its gid counterpart, with no significant changes in the amounts of LHCII and LHCI proteins relative to the PSII and PSI cores except for Lhca4 and Lhca6, which showed a decreased accumulation (Figure 6B). In contrast, when grown in dim light yid-BF3 was markedly different from gid-BF3 (Figure 6B). Whereas CP26 and CP29 accumulated to levels similar to those in the wild-type, all LHCII types I, II (Lhcbm5), III, and IV showed a much decreased accumulation (Figure 6A). The contrast was even higher for the LHCI content. When loading similar contents in PSI cores from whole-cell protein extracts, most of the Lhca proteins were absent from yid-BF3 with only trace amounts of Lhca1, Lhca8, and Lhca9 still being detected (Figure 6B). It is of note that PsaN, PsaG, and PsaK also decreased in yid-BF3. This extensive change in the overall content in PSI-associated proteins prompted us to measure the functional PSI antenna size in yid-BF3 relative to that in the wild-type. To do so, however, we could not use an ECS measurement as a reliable indicator of PSI excitation in yid-BF3 owing to its extensive loss in antenna proteins that contribute to the buildup of the ECS signal. Instead, in this strain we studied the light intensity dependence of PSI charge separation by recording direct P700 oxidation in yid-BF3 mutant as the difference between 430 nm and 445 nm absorption changes (500 ns after a flash). We obtained a good signal-to-noise ratio in this spectral region owing to the low chlorophyll content of this strain (Guergova-Kuras et al., 2001). The resulting saturation curve was compared with the saturation curve for the regular ECS signal in the wild-type (100 μs after a flash in the presence of hydroxylamine and DCMU to eliminate the contribution of PSII). We used the same range of light intensities provided by the same laser flash using the same spectrophotometer for the P700 and ECS saturation curves (see Methods for details). A typical experiment is shown in Figure 7B, and the deduced PSI antenna sizes from three biological replicates are shown in Figure 7A. We observed a loss of 30% in PSI antenna size in yid-BF3 grown under very dim light, which should be compared with the 1.6-fold increase in PSI antenna size when using gid-BF3 grown in the same condition (Figure 4). Estimates of the relative PSII antenna size in yid-BF3, deduced from the half-time in its fluorescence rise relative to that in the wild-type, were consistent with the aforementioned biochemical analysis of its content in LHCII and minor peripheral antenna proteins. It was about half the wild-type PSII antenna size when yid-BF3 was grown in moderate light, similar to the gid-BF3 phenotype, but showed a further decrease in PSII antenna size when grown in dim light, being only about 25% of that in the wild-type (Figure 7A). To assess whether the main features of yid-BF3 grown in dim light indeed were due to the absence of Chl *b* and not merely to the yid phenotype, we recorded similar parameters for a yid-control strain grown in dim light. This strain showed higher chlorophyll content per cell, higher fluorescence yield per cell, and higher F_V/F_M than the yid-BF3 (Table 2). In addition, it retained much larger PSII and PSI antenna sizes than those in the yid-BF3 (Figure 7A and 7C). These observations are consistent with the extensive accumulation of LHCIs and LHCIIs in wild-type and yid-control cells as shown in Supplemental Figure 2. Thus, the most distinct features of yid-BF3 under dim light relative to the wild-type were due to the absence of Chl *b*.

The decreased LHCI content in yid-BF3 grown in dim light could reflect a higher sensitivity to proteolytic degradation of the Chl *b*-lacking antenna proteins in the yid context. We thus placed yid-BF3 in a proteolytic-deficient context by crossing it to the *ftsh1-1* mutant that shows compromised activity of the thylakoid-located FtsH protease (Malnoë et al., 2014). The resulting mutant, yid-BF3-*ftsh1*, had a much lower chlorophyll content than that of yid-BF3 when grown in dim light (Table 2).

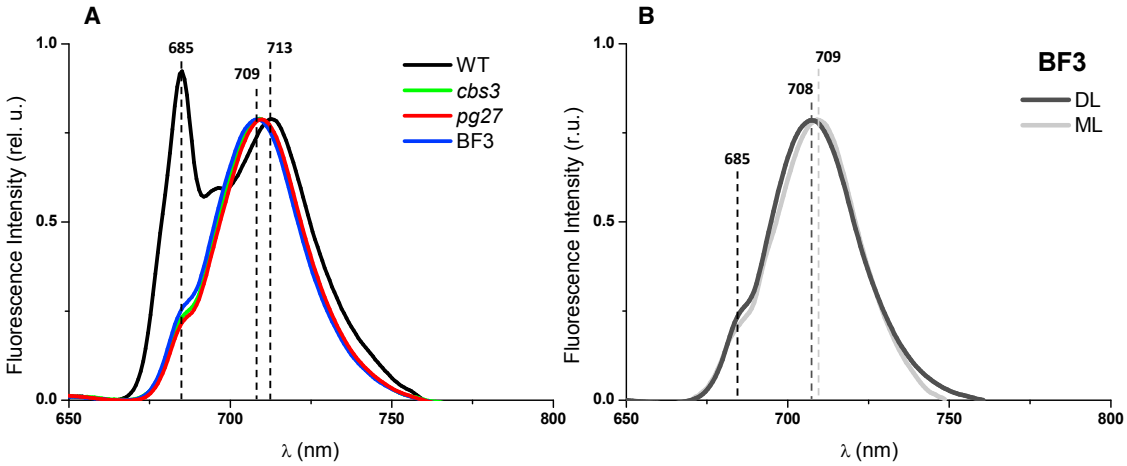

Figure 3. Low-Temperature (77 K) Fluorescence Emission Spectra.
(A) Wild-type (WT) and Chl *b*-less mutants (*cbs3*, BF3, and *pg27*) grown in moderate light (50 μmol photons m^{-2} s^{-1}).
(B) BF3, Chl *b*-less mutant green-in-the-dark, grown under dim light (DL; 1–2 μmol photons m^{-2} s^{-1}) and moderate light (ML; 50 μmol photons m^{-2} s^{-1}).

Its relative chlorophyll deficiency was even more pronounced when grown at moderate light intensity, yielding a very low-fluorescence phenotype under both light regimes for growth. Its F_V/F_M ratio was particularly low, with little if any evidence for PSII activity in very dim light. Consistent with these characteristics, Figure 6A shows that most of the PSII peripheral antenna collapsed in the yid-BF3-*ftsh1* at both dim and moderate light intensity for growth. Only the minor antenna complexes, CP26 and CP29, were preserved at wild-type levels in these mutated contexts. In contrast, when we analyzed LHCI proteins in the double mutant grown in dim light, all LHCI proteins except Lhca4 were detected at a wild-type level (Figure 6B). Thus the decreased level of LHCI proteins in yid-BF3 grown in dim light can be ascribed to their increased degradation by FtsH. yid-BF3-*ftsh1* also accumulated PsaG and PsaK above wild-type levels in contrast to yid-BF3, which was defective for these PSI subunits at dim light. Only PsaN remained insensitive to the inhibition of FtsH, since its level was lower in yid-BF3-*ftsh1* than in yid-BF3. In addition, Lhca3, Lhca7, and Lhca9 accumulated above wild-type levels in yid-BF3-*ftsh1* whereas the other Lhca proteins were at close to wild-type level. The restoration of a wild-type complement of most LHCI proteins in yid-BF3-*ftsh1* grown in dim light was accompanied by restoration of a larger PSI functional antenna, as shown in Figure 7. However, when fitting the data with a mono-exponential function, we noted a marked heterogeneity in the saturation of PSI charge separation in the two mutants. The saturation curves were better fitted with two exponentials (Figure S3), which disclosed an even larger heterogeneity in the yid-BF3-*ftsh1* mutant. Thus, FtsH inactivation, although it leads to an increased accumulation of most LHCI proteins in the absence of Chl *b*, does not allow all PSI centers to restore a wild-type antenna size.

The 77 K emission spectra were recorded for yid-BF3 and the two other yid-Chl *b*-less mutants grown in dim light or moderate light (Figure 8). In contrast to their gid counterparts, the emission spectra of the three yid-Chl *b*-less mutants resembled that of the wild-type in dim light, inasmuch as they displayed the regular PSII emissions peaks at 685 nm and 695 nm, and a PSI emission peak in the 713–715 nm region. However, it is of note that the PSI peak was higher, relative to the PSII peaks, than in the wild-type grown in the same light conditions. When the yid-Chl *b*-less mutants were grown in moderate light, their 77 K emission spectra now resembled that of their gid counterparts with a major emission peak at 709 nm and a shoulder at 685 nm. The comparison of the biochemical patterns and 77 K emission spectra of the yid versus gid Chl *b*-less mutants shows that the 709 nm peak requires sustained Chl *a* synthesis (see Discussion).

Biochemical Purification of Chlorophyll–Protein Complexes from yid-BF3

We separated three chlorophyll–protein complexes from wild-type thylakoid extracts on sucrose gradient, as previously reported (Sugimoto and Takahashi, 2003). As shown in Figure 9A, the three bands were detected from wild-type grown in dim and moderate light. A1, A2, and A3 mainly contain LHCIIs, PSII core complexes, and PSI–LHCI supercomplexes, respectively. A broad green band, A3′, which contained CP26, CP29, and Lhcbm5 (LHCII type II), was detected below A3 or A3* (Figure 9A and 9B). In contrast, A3 was scarcely detected from yid-BF3 grown in dim light, which can be expected from the results in Figure 6B showing that LHCIs accumulate to a very low level in such growth conditions. Instead a broad A2 band was obtained, in which the PSI core complex as well as the PSII core complex were separated (Ozawa et al., 2010). A1 band, which was slightly upshifted on the gradient, was broader and weaker than in the wild-type, as expected from the biochemical data from whole cells in Figure 6. When the proteins were separated and stained, LHCII type I and type III bands were scarcely detected and LHCII type IV band was rather poor despite the presence of the substantial amount of green band as A1 (Figure 9B). Immunoblot also confirmed that LHCII type I and type III bands were not detectable and LHCII type IV band was faint (Figure 10). Since Figure 6A shows that a substantial amount of LHCII proteins was detected in the total cell protein extracts from yid-BF3 cells grown in dim light,

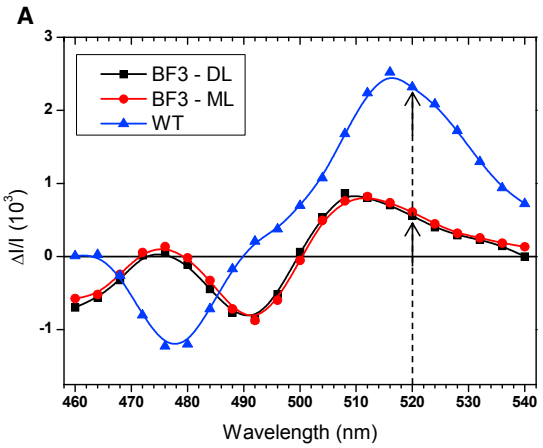

B

Parameter			WT	BF3
PSII	$1/t_{1/2}$ *fluorescence rise* *(DCMU)*	DL	1.0	0.41 ± 0.02
		ML	1.0	0.57 ± 0.07
PSII	$1/I_{2/3}$ *flash induced ECS* *DCMU+HA sensitive*	DL	1.0	0.4 ± 0.1
		ML	1.0	0.5 ± 0.1
PSI	$1/I_{2/3}$ *flash induced ECS* *DCMU+HA insensitive*	DL	1.0	1.6 ± 0.2
		ML	1.0	1.10 ± 0.07
PSII / PSI		DL	1.37 ± 0.03	1.4 ± 0.2
		ML	1.01 ± 0.04	1.22 ± 0.09

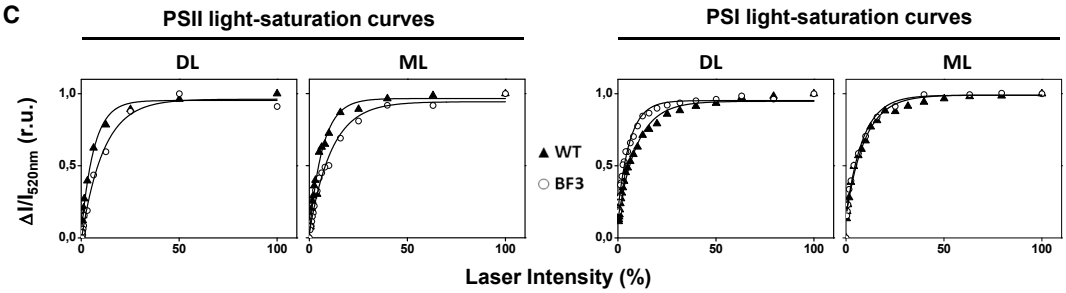

Figure 4. Electrochromic Shift Spectra and Photosystem II and Photosystem I Relative Antenna Size.

(A) Electrochromic shift (ECS) spectra. The absorption change was measured 100 μs after the actinic flash hitting 100% of centers. WT, wild-type.

(B) Photosystem II (PSII) and photosystem I (PSI) relative antenna size and ratio PSII/PSI in BF3 strain (Chl *b*-less mutant). PSII antenna size was estimated (i) from F_M saturation kinetic ($1/t_{1/2}$) in the presence of DCMU (10^{-5} M) and (ii) spectroscopically from the light-saturation curves of the ECS changes at 520 nm ($1/I_{2/3}$). We measured the amplitude of the fast phase (100 μs) of the ECS signal upon excitation with a saturating laser flash in the presence or absence of the PSII inhibitors (DCMU + hydroxylamine [HA]). The data presented are expressed here after normalization to the antenna size measured in the wild-type (WT), which is set to a value of 1. All values represent means ± SD (n = 3–5). DL, dim light (1–2 μmol photons m^{-2} s^{-1}); ML, moderate light (50 μmol photons m^{-2} s^{-1}).

(C) PSII and PSI light-saturation curves from their ECS signal, recorded 100 μs after one single turnover flash, in the wild-type (WT; solid triangles) and the BF3 mutant (open circles).

together with an LHCII-green band A1 after thylakoid solubilization, we conclude that the LHCII proteins were attacked by proteinases despite the use of protease inhibitors during the purification procedure. Although the holocomplexes were still maintained, the upshift of A1 suggests that their structure has been modified in the absence of Chl *b*.

When we grew yid-BF3 in moderate light, A1 increased to nearly wild-type level. A significant amount of LHCII proteins was also detected in A1 (Figure 9A and 9B), indicating that LHCII apoproteins were protected from proteinase digestion. The amount of A2 significantly decreased but remained higher than that in the wild-type. It is of note that a weak and slightly upshifted A3 (designated as A3* in Figure 9A) was observed. The upshift is ascribed to a modification of the PSI–LHCI structure because A3* lost some LHCI polypeptides (Figure 9B). The immunoblots of Figure 10 clearly indicate that Lhca2, Lhca3, Lhca7, Lhca8, and Lhca9 were present at substantial levels (0.42 ± 0.08, 0.71 ± 0.16, 0.42 ± 0.14, 0.71 ± 0.26, and 0.31 ± 0.07 on a PSI basis [mean and SD, n = 3]). Lhca1 and Lhca6 were weakly detected (0.08 ± 0.04 and 0.13 ± 0.02 on a PSI basis [mean and SD, n = 3]), whereas Lhca4 and Lhca5 were below detection level in A3*. However, we note that A3* is contaminated by A2, which contains PSI core without LHCI proteins, which underestimates the levels of LHCI proteins in PSI–LHCI in A3*. The contrasting stability of the nine LHCI proteins in PSI–LHCI supercomplexes probably originates from their different localization in PSI–LHCI supercomplex (Drop et al., 2011).

DISCUSSION

To gain an in-depth understanding of the impact of Chl *b* deficiency on the function, assembly, and stability of antenna complexes, LHCIs, and LHCIIs, we analyzed Chl *b*-less mutants, *pg27*, *cbs3*, and BF3, of the green alga *C. reinhardtii*. As previously reported (Tanaka et al., 1998), *cbs3* has a large deletion of several genes in a genomic region containing the *CAO* gene responsible for Chl *a* to Chl *b* conversion. Here we showed that the *pg27* and BF3 mutants have point mutations in the *CAO* gene that lead to an early termination of its translation. Characterization of these mutants offered clear insights as to how Chl *b* deficiency affects the light-harvesting function, synthesis, and stability of Chl *a*/*b* binding proteins. Here we focused on

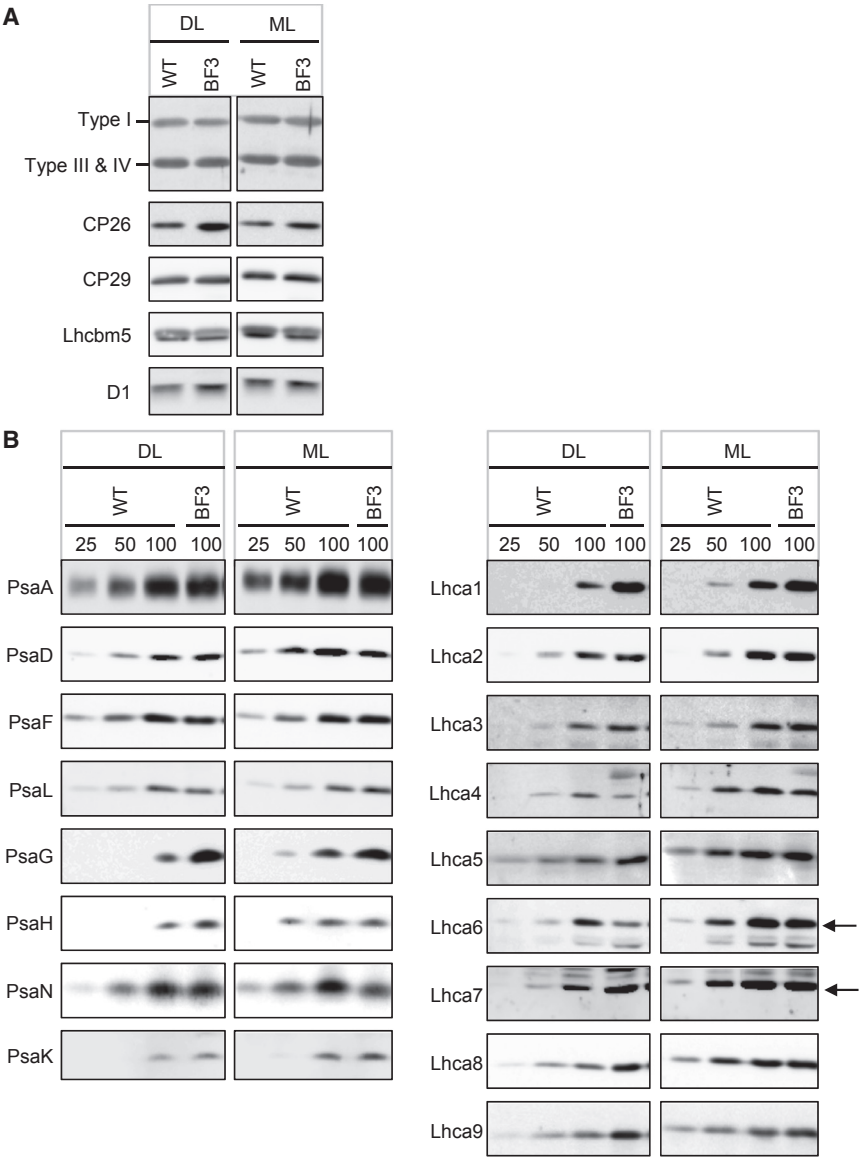

Figure 5. Effects of Growth Light Conditions on LHCI and LHCII Accumulation.

Cells were grown in TAP medium under dim light (DL; 2 μmol photons m^{-2} s^{-1}) and moderate light (ML; 50 μmol photons m^{-2} s^{-1}). Total cell proteins were solubilized with 2% SDS and 0.1 M DTT at 100°C for 1 min, and were separated by SDS–PAGE, electroblotted onto a nitrocellulose filter, probed with specific antibodies, and visualized by enhanced chemiluminescence. WT, wild-type. Arrows point to the band representing the actual antigen.

(A) PSII and LHCII proteins. Total cell proteins (0.5 μg Chl) were loaded and probed with antibodies against CP26, CP29, LHCIIs (types I, II [Lhcbm5], III, and IV), and D1 (PsbA). BF3/WT ratio on D1: 1.3 ± 0.2 in DL and 1.1 ± 0.2 in ML (n = 3).

(B) PSI and LHCI proteins on a PSI basis (0.5 μg Chl for WT and BF3 grown in ML; 0.35 μg Chl and 0.44 μg Chl for WT and BF3 grown in DL). The blots were proved with antibodies against PSI proteins (PsaA, PsaD, PsaF, PsaG, PsaH, PsaK, PsaL, and PsaN) and LHCI proteins (Lhca1–9).

the light-harvesting function of LHCs in BF3 cells by spectroscopic measurements and analyzed the accumulation and stability of LHCs using a battery of specific antibodies raised against the major LHCII proteins (types I, II, III, and IV), the minor LHCII proteins (CP26 and CP29), and the LHCI proteins (Lhca1–9).

The Absence of Chlorophyll *b* Does Not Affect Accumulation of LHC Proteins when Chlorophyll *a* Availability Is Unaltered

Previous reports revealed that Chl *b* deficiency in plants did not affect mRNA levels for LHC apoproteins and neither did it alter their translation, but merely their accumulation (Espineda et al., 1999; Nick et al., 2013). These results suggested that Chl *b* is required for efficient assembly and/or proteolytic resistance of the LHC proteins. Here we showed that the nine LHCI proteins from *Chlamydomonas* accumulated to nearly wild-type levels in the Chl *b*-less mutant BF3 grown in moderate light. Moreover, five of these proteins overaccumulated in BF3 cells grown in dim light. On the other hand, the accumulation of the four types of major LHCII proteins (LHCII types I, II, III, and IV) and the two minor LHCII proteins (CP26 and CP29) in BF3 (gid-BF3) cells grown in dim light and moderate light remained similar or only slightly decreased relative to those in the wild-type. In addition, after solubilization of thylakoid membranes and sucrose gradient centrifugation, we observed that assembly of LHCII complexes, which are likely to display new structural features, still occurs in the absence of Chl *b*. Thus, the mere absence of Chl *b* does not compromise the accumulation of the major Chl *a*/*b* binding proteins in the thylakoid membranes of *Chlamydomonas*. This is in contrast to plant chloroplasts, but consistent with the conclusion regarding *Chlamydomonas* chloroplast from Polle et al. (2000) who, at that time, did not have access to a detailed biochemical analysis of the LHC complement in Chl *b*-lacking thylakoid membranes.

Examination of the three-dimensional structures of the major LHCII (Liu et al., 2004) CP29 (Pan et al., 2011), and the four LHCI complexes in PSI–LHCI supercomplex (Mazor et al., 2015; Qin et al., 2015) shows that Chl *a* molecules are located around the two transmembrane helices (helices B and A) that form the central structure. Most Chl *b* molecules, as well as the remaining Chl *a* molecules, are located around helix C that forms the peripheral domain. Since chlorophyll molecules are densely packed in LHC complexes, the deficiency of Chl *b* should modify the structural organization of LHC complexes to some extent, which may increase their susceptibility to proteinases. However, the present study argues for the folding of Chl *a*/*b* apoproteins and the integration of Chl *a* into chlorophyll–protein complexes in a protease-resistant form in the thylakoid membranes in the total absence of Chl *b*. Indeed,

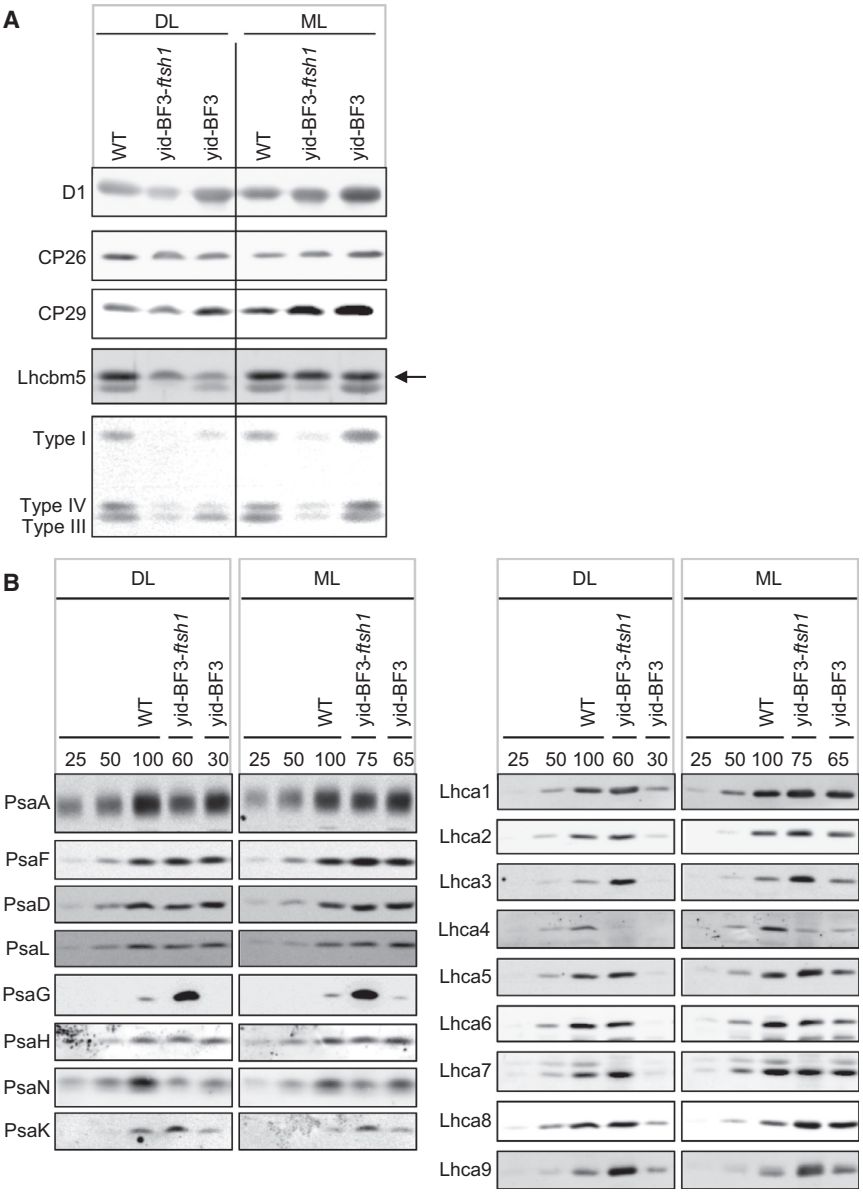

Figure 6. Effects of the yid Background and *ftsh1-1* Mutation on LHCI and LHCII Accumulation.

(A) Accumulation of PSII and LHCII proteins in yid-BF3 and yid-BF3-*ftsh1*. Cells were grown in TAP medium under dim light (DL) and moderate light (ML). Total cell proteins (0.5 μg Chl) were subjected to SDS–PAGE, electroblotted onto a nitrocellulose filter, and proved with antibodies against D1 (PsbA), CP26, CP29, Lhcbm5 (arrow), and LHCIIs (types I, III, and IV). WT, wild-type.

(B) Accumulation of PSI, LHCI proteins in yid-BF3 and yid-BF3-*ftsh1*. Total cell proteins on a PSI basis were subjected to SDS–PAGE and blotted onto a nitrocellulose filter. The filter was hybridized with antibodies against PSI subunits (PsaA, PsaF, PsaD, PsaL, PsaG, PsaH, PsaN, PsaK), LHCI proteins (Lhca1–9), CP26, CP29, and Lhcbm5 (arrow in **A**). WT, wild-type.

reconstitution experiments using overexpressed LHCII apoproteins and pigment extracts led to the conclusion that some Chl *b* binding sites of LHC proteins also can be occupied by Chl *a* with a lower affinity (Bassi et al., 1999). Chl *b* appears critical to maintain a protease-resistant folding of the holocomplex only when these sites remain free of Chl *a* binding, because of its limited availability (see below).

Despite the preserved accumulation of LHC proteins lacking Chl *b*, their functional properties as peripheral antennae for the two photosystems were largely modified. The antenna size of PSII was two times smaller than that in the wild-type, despite the near to wild-type accumulation of the apoproteins. There was a drastic drop in F_V/F_M and a new 77 K emission peak at 708–709 nm, both of which suggest decreased energy transfer efficiency to the PSII reaction centers. In contrast, the absence of Chl *b* did not alter the efficiency of light harvesting within the LHCI antenna as demonstrated by the wild-type accumulation of Lhca proteins and a PSI antenna size similar to that of the wild-type in gid-BF3 cells grown in moderate light. It is of interest that the functional antenna size for PSI in gid-BF3 grown in dim light was even larger than that in wild-type (Figure 4C). In fact gid-BF3 accumulated most LHCI proteins, except for Lhca4 and Lhca6, at higher levels than wild-type. Whereas LHCII amounts vary in response to light environmental changes (Anderson, 1986), it was until now considered that the accumulation and topology of LHCI proteins in PSI–LHCI supercomplex were rather static. LHCI proteins associate with the PSI core complex at specific binding sites and in a seemingly stoichiometric manner (Drop et al., 2011). Since the extra LHCI proteins efficiently function in light harvesting for the PSI reaction center, they should occupy alternative binding sites to the PSI complex. We suggest that the distal site at which PsaI/PsaL/PsaH are present, where monomers from minor LHCII antenna complex, which display Chl *a*/Chl *b* ratios similar to those of LHCI proteins, may bind to PSI upon transition to state 2 (Takahashi et al., 2006), could be occupied by the extra LHCI proteins in the Chl *b*-less mutants. This could result from a lower ability of the PSII peripheral antenna proteins lacking Chl *b* to visit these PSI binding sites in the Chl *b*-less mutants. Thus, we conclude that the accumulation of LHCI proteins with respect to the PSI core complex may be regulated, at least in part, by the presence of Chl *b*, possibly through competition for the binding sites of Chl *b*-lacking minor LHCII proteins.

The Absence of Chl *b* Significantly Destabilizes LHC Complexes when Chl *a* Synthesis Is Limited

Mutants with a yid phenotype spontaneously arise when *Chlamydomonas* is kept in laboratory conditions. Besides three

Parameter		WT	yid	yid-*cbs3*	yid-*pg27*	yid-BF3	yid-BF3-*ftsh1*
[Chl] (μg/10^6 cell)	DL	1.2 ± 0.2	0.49 ± 0.09	0.41 ± 0.05	0.25 ± 0.03	0.39 ± 0.03	0.19 ± 0.02
	ML	2.0 ± 0.3	2.1 ± 0.3	1.2 ± 0.1	1.3 ± 0.2	1.2 ± 0.3	0.32 ± 0.04
Chl *a*/*b*	DL	2.9 ± 0.2	3.0 ± 0.2	–	–	–	–
	ML	3.1 ± 0.1	3.4 ± 0.2	–	–	–	–
F_M/cell	DL	100%	54% ± 6%	8% ± 2%	11% ± 2%	12% ± 5%	15% ± 4%
	ML	100%	98% ± 14%	31% ± 5%	32% ± 4%	29% ± 3%	18% ± 3%
F_V/F_M	DL	0.75 ± 0.02	0.64 ± 0.03	0.42 ± 0.05	0.47 ± 0.05	0.38 ± 0.06	0.07 ± 0.04
	ML	0.75 ± 0.01	0.71 ± 0.03	0.38 ± 0.08	0.3 ± 0.1	0.3 ± 0.1	0.18 ± 0.08

Table 2. Chlorophyll and Fluorescence Parameters of Wild-Type (WT), Yellow-in-the-Dark Control Strain (yid), Chl *b*-Less Mutants in Yellow-in-the-Dark Background (yid-*cbs3*, yid-*pg27*, and yid-BF3), and Double Mutant Yellow-in-the-Dark (yid-BF3-*ftsh1*).
Chlorophyll concentrations were determined according to Porra et al. (1989). Percentage was determined by comparison of the mutant with the wild-type cells grown under the same light condition. Values represent means ± SD (n = 3–10). DL, dim light (1–2 μmol photons m^{-2} s^{-1}); ML, moderate light (50 μmol photons m^{-2} s^{-1}).

chloroplast loci controlling the greening process in the dark, at least seven nuclear loci have been identified so far (Sager, 1955; Hudock and Levine, 1964; Ford and Wang, 1980a, 1980b; Cahoon and Timko, 2000). These mutants are impaired in the chlorophyll biosynthesis pathway in darkness but display a wild-type phenotype when placed under illumination, because of the presence of an alternative pathway for chlorophyll biosynthesis in the light. Thus Chl *a* availability is light intensity dependent in the yid strains. Indeed, yid-BF3 cells are pale green when grown in dim light as they synthesize less Chl *a*. When they are grown at medium light intensity, they produce three to five times larger amounts of chlorophyll per cell (Table 2). This boosts the accumulation of chlorophyll-binding proteins and places them in a similar situation as their gid counterparts. Thus, it is in dim light only that the yid situation disclosed new features of the Chl *b*-less phenotype. Here we showed that the accumulation level of LHCI proteins was significantly decreased in yid-BF3 compared with that in gid-BF3 when grown in dim light. Since yid-control cells accumulated LHCI proteins almost normally even when grown in dim light (Supplemental Figure 2), the presence of Chl *b* must be essential to form a protease-resistance structure of LHCI proteins. However, higher levels of LHCI complexes were restored when the yid-BF3 mutant was grown in moderate light. Taken together these observations suggest that, under limiting light conditions for growth, the amount of Chl *a* synthesized in yid-BF3 cells is too limited to integrate Chl *a* into Chl *b* binding sites in LHC complexes, which results in their degradation. Indeed, we observed that the inactivation of FtsH restored a larger LHCI antenna complement in dim light. Thus the LHCI proteins should be regarded as a new class of genuine FtsH substrates, in addition to PSII and cytochrome b_6f complexes that were previously identified as FtsH sensitive in *Chlamydomonas* (Malnoë et al., 2014; Wei et al., 2014). Strangely enough, LHCII proteins under the same conditions remained FtsH insensitive. Their amount in the yid-BF3 context looked even lower when the protease was inactivated. However, this was due in part to their loading on a chlorophyll basis, because yid-BF3-*ftsh1* is enriched in LHCI proteins.

The contrasting FtsH sensitivity of LHCI and LHCII proteins, which are homologous proteins, may arise from their distinct localization in the thylakoid membranes. LHCII proteins are in stacked membranes at a distance from FtsH in unstacked membranes where LHCI proteins also reside (Fristedt et al., 2009). In this context another proteolytic system would be responsible for LHCII protein degradation, such as the Deg proteases that can act from the lumen side of the membranes where they should have access to the stacked membrane domains (Schuhmann and Adamska, 2012). It is of note that FtsH inactivation in *Chlamydomonas* prevents PSII repair (Malnoë et al., 2014) as it does in cyanobacteria and plant chloroplasts (for a review see Yoshioka-Nishimura and Yamamoto, 2014). These observations point to a high sensitivity of FtsH mutants to photodamage, and are most likely to account for the huge decrease in PSII activity. This accumulation of dysfunctional PSII certainly keeps high rates of reactive oxygen species (ROS) production under illumination. These ROS may be responsible for the loss in LHCII proteins and the further loss in chlorophyll per cell at the two light regimes for growth of the yid-BF3-*ftsh1* mutant.

Deficiency of Chl *b* Destabilizes PSI–LHC Supercomplex

PSI–LHCI supercomplex containing the nine LHCI complexes could not be recovered from yid-BF3 cells grown under moderate light, although PSI light-saturation curves indicated efficient energy transfer from LHCI to PSI reaction centers, with a wild-type level of accumulation of most LHCI proteins in the thylakoid membranes. The separated PSI–LHCI subcomplex (A3*) lacked Lhca1, Lhca4, and Lhca5 and contained only a small amount of Lhca1 and Lhca6. In fact the position of A3* on sucrose density gradient was upshifted compared with that of A3 from wild-type cells, indicating that the size is smaller than that of the wild-type complex. These results suggest that LHCI complexes are functionally associated with the PSI core complex in the chloroplast but that their association is impaired during solubilization and/or purification in the absence of Chl *b*. The three-dimensional structure of a plant PSI–LHCI supercomplex indicates that each LHCI complex in the supercomplex interacts with its neighboring LHCI complex through a domain of helix C (Drop et al., 2011). Since this domain associates most Chl *b*, the structure responsible for the stable LHCI association in PSI–LHCI supercomplex should be modified in the absence of Chl *b*. We noted that substantial amounts of Lhca2, Lhca3,

A

Parameter			yid-BF3	yid-BF3-*ftsh1*	yid
PSII	$1/t_{1/2}$ *fluorescence rise* *(DCMU)*	DL	0.25 ± 0.06	-	0.73 ± 0.02
		ML	0.6 ± 0.1	0.31 ± 0.01	0.90 ± 0.02
PSI	$1/I_{2/3}$ *charge separation* *(DCMU + HA)*	DL	0.7 ± 0.1	0.93 ± 0.06	1.29 ± 0.06

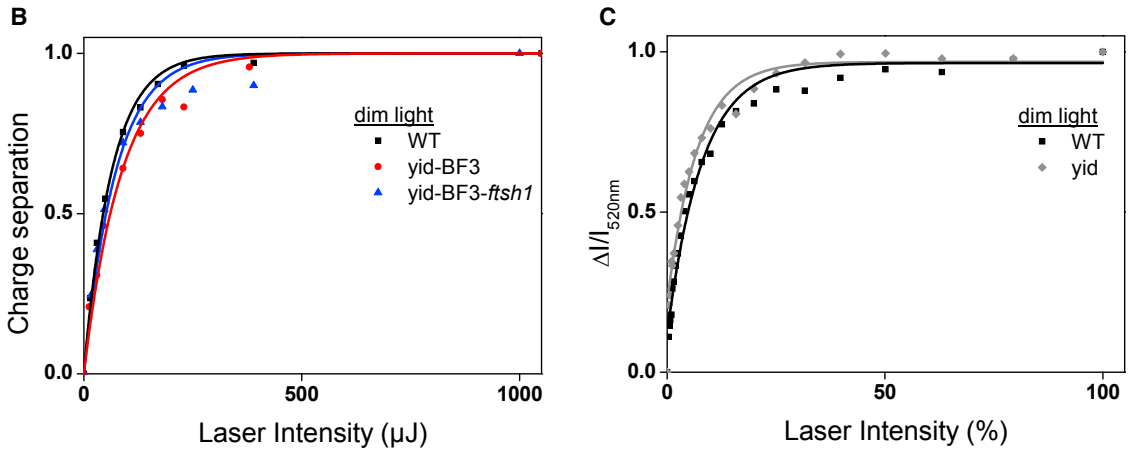

Figure 7. Photosystem II and Photosystem I Relative Antenna Size in Wild-Type, Yellow-in-the-Dark Strain Control (yid), Yellow-in-the-Dark Chl *b*-Less Mutant (yid-BF3), and Double Mutant (yid-BF3-*ftsh1*).

(A–C) PSII antenna size **(A)** has been estimated from F_M saturation kinetic ($1/t_{1/2}$) in the presence of DCMU (10^{-5} M). PSI antenna size has been estimated spectroscopically, in the presence of the PSII inhibitors (DCMU + hydroxylamine [HA]). We measured the light-saturation curves of the P700 oxidation signal in the blue region of the spectrum for yid-BF3 and yid-BF3-*ftsh1* **(B)** or of the contribution of PSI charge separation to the ECS signal for the yid-control strain **(C)**.

All data presented are expressed after normalization to the antenna size measured in the wild-type (WT) under the same light condition. Data from **(B)** and **(C)** are fitted with a mono-exponential function. All values from **(A)** represent means ± SD (n = 3). DL, dim light (1–2 µmol photons m^{-2} s^{-1}); ML, moderate light (50 µmol photons m^{-2} s^{-1}).

Lhca7, Lhca8, and Lhca9 remained associated with PSI core complex in A3* fraction. This strongly suggests that these LHCI proteins are more tightly bound to PSI core complex.

It has been proposed that Lhca3 has direct contact with PsaK (Naumann et al., 2005), and Lhca2 and Lhca9 are located in proximity to PsaG (Drop et al., 2011), which may stabilize the association of these LHCI proteins to the PSI core complex or protect them from proteinase digestion. Indeed, we noted that PsaK and PsaG were labile in yid-BF3 in which Lhca2 and Lhca9 were reduced (Figure 6B), but they overaccumulated in gid-BF3 when Lhca3 and Lhca9 are present at a higher level than in wild-type cells (Figure 5B). This suggests that the two PSI and LHCI subunits show a concerted accumulation in the thylakoid membranes, consistent with their close interaction in the PSI–LHCI supercomplex. A higher susceptibility of the two PSI subunits to the action of the FtsH protease in the absence of Lhca3 and Lhca9 may account for this concerted accumulation.

The nine LHCI proteins are located on one side of the PSI core complex, forming two layers (Drop et al., 2011) in wild-type cells. LHCI proteins from the inner layer directly bind to PSI core complex and are sandwiched by those LHCI proteins from the outer layer. This layer organization suggests that LHCI proteins located in the inner layer should be better associated with PSI cores and better protected from proteinase digestion. Thus, it is inferred that Lhca2, Lhca3, Lhca7, Lhca8, and Lhca9 would be located in the inner layer while the others, Lhca1, Lhca4, Lhca5, and Lhca6, would be part of the outer layer.

A New Type of Antenna Complex Synthesized in Chl *b*-Less Mutant

The Chl *a* binding peripheral antenna proteins that accumulate in the absence of Chl *b* generate a new type of chlorophyll–protein complex readily identified by its 77 K fluorescence emission spectrum that peaks at 708–709 nm. This is a spectral region similar to that of isolated LHCI, which has a much higher Chl *a*/Chl *b* ratio than LHCII in the wild-type genetic context (Figure 8). That LHC proteins, whether from LHCI or LHCII, emit fluorescence in this spectral region when binding only Chl *a* is further substantiated by our observation that this emission peak diminishes together with the LHCI and LHCII proteins when

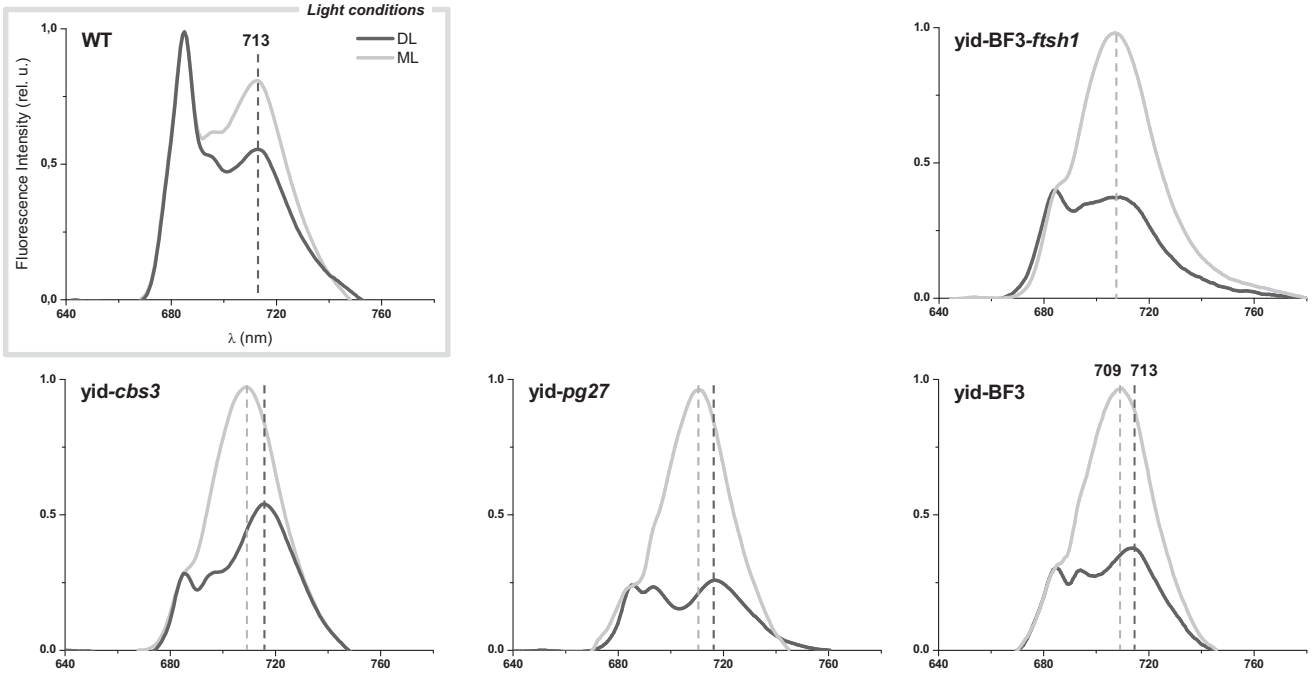

Figure 8. Low-Temperature (77 K) Fluorescence Emission Spectra in the yid Mutants.
Low-temperature (77 K) fluorescence emission spectra of cells of wild-type control (WT), Chl *b*-less mutants yellow-in-the-dark (yid-*cbs3*, yid-BF3, and yid-*pg27*), and double mutant in yid context (yid-BF3-*ftsh1*) grown under dim light (DL; 1–2 μmol photons m^{-2} s^{-1}) and moderate light (ML; 50 μmol photons m^{-2} s^{-1}).

yid-BF3 is grown in dim light, whereas the two are present in gid-BF3 grown in the same conditions. Interestingly, the 708–709 nm peak is not restored in the yid-BF3-*ftsh1* mutant when grown in dim light, despite the accumulation of LHCI proteins binding only Chl *a*. However, LHCII type I, III, and IV proteins also remained very low in the yid-BF3-*ftsh1* mutant in the two light regimes for growth (Figure 6), whereas the 709 nm emission arose only in moderate light. In contrast, CP29 and LHCII type II (Lhcbm5) increased significantly from dim to moderate light condition in yid-BF3-*ftsh1*. We observed a similar behavior in the yid-BF3 strain. These observations strongly suggest that the sole minor LHCII proteins, when binding only Chl *a*, are responsible for this new emission peak. However, we noted that gid-BF3 (not shown) and yid-BF3 (Supplemental Figure 4) grown in dim light and moderate light showed only a 77 K fluorescence peak at 683–685 nm in those fractions corresponding to isolated LHCII complexes (A1 fraction), which contains major LHCII types I, III, and IV. Similarly only a 683–685 nm emission peak was visible in the A3′ fraction, which contains minor LHCII (CP26 and CP29) and LHCII type II as well as PSI proteins. After separation of chlorophyll–protein complexes, we could not find any other green fraction that emitted a 77 K fluorescence peak at 708–709 nm. Thus, we hypothesize that the 708–709 nm emission peak originates from those Chl *a* that occupy Chl *b* binding sites in the PSII peripheral antenna and are loosely bound to the apoproteins. They would be lost during membrane solubilization and/or purification of the chlorophyll–protein complexes. Because such Chl *a*-only antenna proteins emit their 77 K fluorescence at longer wavelengths than the PSII cores, this suggests that they would be less efficient in energy transfer to the PSII reaction centers at room temperature. In agreement with this conclusion, we observed that the PSII functional antenna size in the Chl *b*-less mutants remains much smaller than in the wild-type control despite the immunodetection of LHCII proteins and minor antenna complexes in wild-type amounts in the mutants whatever the light intensity for growth in the gid-BF3 mutant. Thus, these antenna complexes transfer energy poorly to the PSII cores even at room temperature, where they may act as quenchers of PSII excitation.

METHODS

Strains and Growth Conditions

Wild-type and mutant strains of *C. reinhardtii* were grown mixotrophically at 25°C in Tris-acetate-phosphate (TAP) medium (pH 7.2) (Harris, 2009), on a rotary shaker (150 rpm) either in darkness or under continuous light (2 or 50 μmol photons m^{-2} s^{-1}). The mutant strains, devoid of chlorophyll *b*, which were used in the present study, have been described previously: *cbs3* (Tanaka et al., 1998), BF3 (de Vitry and Wollman, 1988), and *pg27* (Picaud and Dubertret, 1986). Before being further characterized, these mutants were backcrossed to either WT.T222mt$^+$ or WTS24 mt$^-$, derived from wild-type 137c, that we use as reference strains in our laboratory. The yellow-in-the-dark strain control (yid) was obtained by crossing yid-BF3 mt$^+$ with WTS24 mt$^-$ and the yid-BF3-*ftsh1* strain by crossing yid-BF3 mt$^+$ with mutant strain *ftsh1-1* mt$^-$ (Malnoë et al., 2014), and progenies were selected by PCR, according to Malnoë et al. (2014), and by their fluorescence properties. Crosses were performed according to Harris (2009).

Sequencing of *CAO* Gene

Wild-type and mutant genomic DNA was amplified by PCR using four couples of primers along the *CAO* gene. All amplification products were

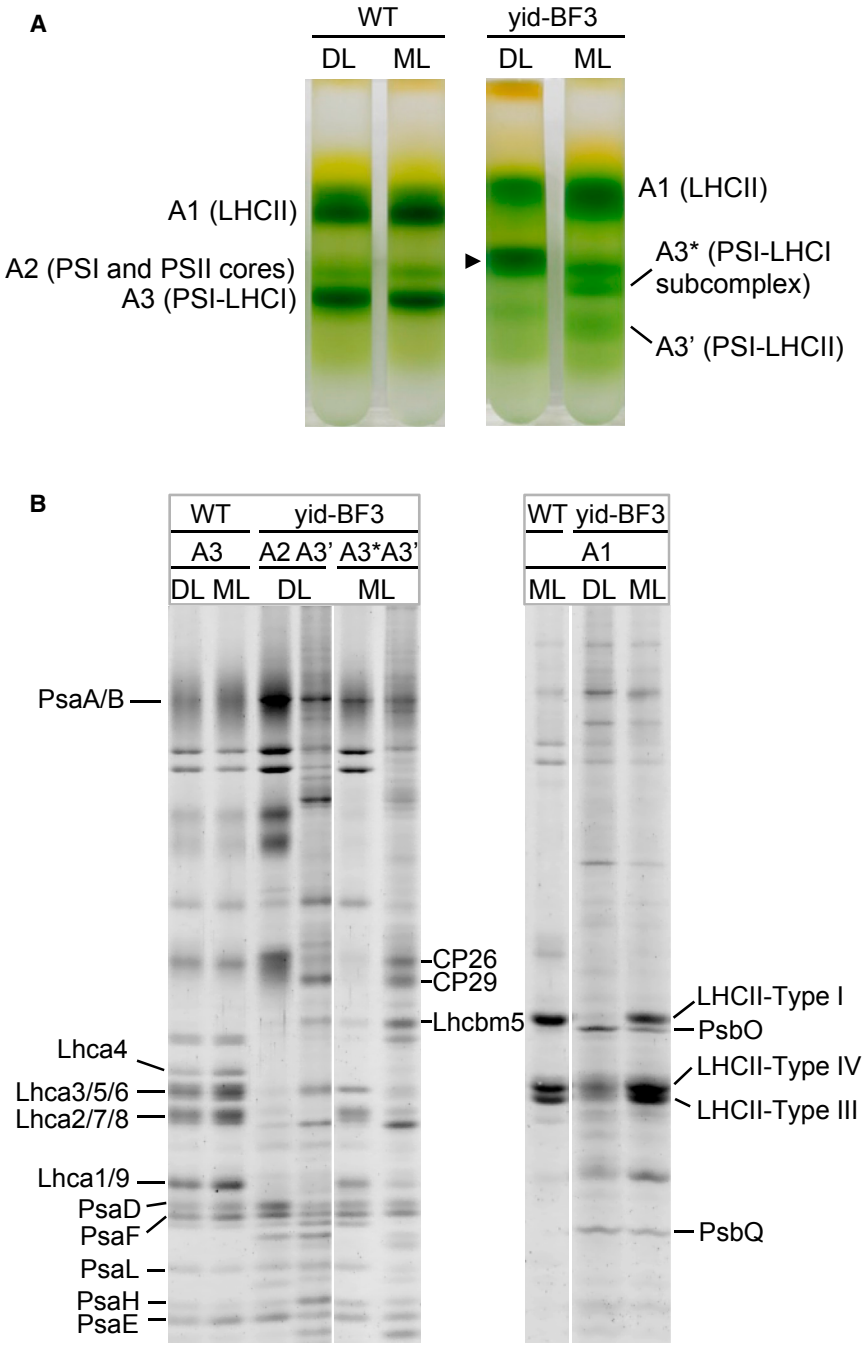

Figure 9. Separation of Chlorophyll–Protein Complexes.

(A) Thylakoid membranes isolated from wild-type (WT) and yid-BF3 cells under dim light (DL) and medium light (ML) were solubilized with 2.0% (w/v) DM on ice for 15 min and separated by sucrose density gradient ultracentrifugation. A1, A2, and A3 contain LHCII, PSI, and PSII cores, and PSI–LHCI supercomplex from WT. A1, A2 (indicated by arrowhead), and A3′ were separated from yid-BF3 grown under DL, whereas A1, A2, A3*, and A3′ were separated from yid-BF3 grown under ML.

(B) Polypeptides of PSI and LHCI in A3 from wild-type (WT) grown under DL and ML and of A3′ from yid-BF3 grown under DL and A3* and A3′ from yid-BF3 grown under ML were compared (left). Polypeptides of LHCI and LHCII in A1 of WT grown under ML and of yid-BF3 grown under DL and ML were compared (right). Five and ten microliters of the fractions from WT and yid-BF3, respectively, were loaded in each lane.

purified and then sequenced (Eurofins). Primers used for PCR and sequencing are listed in Supplemental Table 1.

Complementation of BF3 Mutant

The *CAO* gene was amplified from wild-type *Chlamydomonas* genomic DNA. Primers used for amplification of the genomic sequence annealed to regions 880 bp upstream of the *CAO* transcription start site (5′-AGGGGGCACTGTCGGTACAG-3′) and 342 bp downstream of the 3′ UTR (5′-GCGAGGCGCCAATGCTACCT-3′). BF3 mutant cells were grown in TAP medium at 20 μmol photons m^{-2} s^{-1} to early exponential phase (1×10^6 cells ml^{-1}) and collected by centrifugation at room temperature at 4000 rpm for 7 min, then the cell pellet was resuspended in TAP medium containing 40 mM sucrose (ToS) to a final cell concentration of 1×10^8 cells ml^{-1}. The *CAO* PCR product (500 ng) plus 40 μg of salmon sperm DNA and 160 ng of the *AphVIII* gene was incubated with BF3 cells at 16°C for 20 min. The cells were electroporated at 1 kV and 10-μF capacitance and then incubated at 16°C. After 30 min of incubation, cells were diluted in 5 ml of ToS medium. The electroporated cultures were incubated overnight under dim light (2 μmol photons m^{-2} s^{-1}) with gentle agitation, then spread on solid TAP medium containing 10 μg ml^{-1} paromomycin and 100 μg ml^{-1} ampicillin and placed in the dark. After 2 weeks of growth in the dark, only transformants harboring the introduced *CAO* gene were dark green and highly fluorescent.

Preparation of Cells and Thylakoid Membranes, and Separation of Chlorophyll–Protein Complexes

For analysis of cell proteins, wild-type and mutant cells grown to a mid-log phase in TAP medium were harvested by centrifugation and suspended in medium containing 50 mM Tris–HCl (pH 8.0) and 20% (w/v) glycerol at 0.25 mg Chl ml^{-1}. Thylakoid membranes were isolated in the presence of protease inhibitors, 1 mM PMSF, and EDTA according to Chua and Bennoun (1975) with some modifications as described by Takahashi et al. (1991). The thylakoid membranes were solubilized with 2.0% (w/v) *n*-dodecyl-β-D-maltoside (β-DM) in the presence of protease inhibitor cocktail (Complete, Roche), and the thylakoid extracts were loaded on linear sucrose density gradient from 0.1 to 1.3 M sucrose containing 5 mM Tricine–NaOH (pH 8.0) and 0.05% DM. Ultracentrifugation was performed on a swinging bucket rotor SW41Ti (Beckman) at 288 000 *g* for 16 h (Sugimoto and Takahashi, 2003). The resulting gradients were fractionated from the bottom to the top.

Analyses of Polypeptides

Total cell proteins and polypeptides in fractions from sucrose density gradient were solubilized in the presence of 2% SDS and 0.1 M dithiothreitol (DTT) at 100°C for 1 min and at 80°C for 3 min, respectively, then separated by SDS–PAGE. To optimize separation of polypeptides we employed four different electrophoresis systems; a standard system by

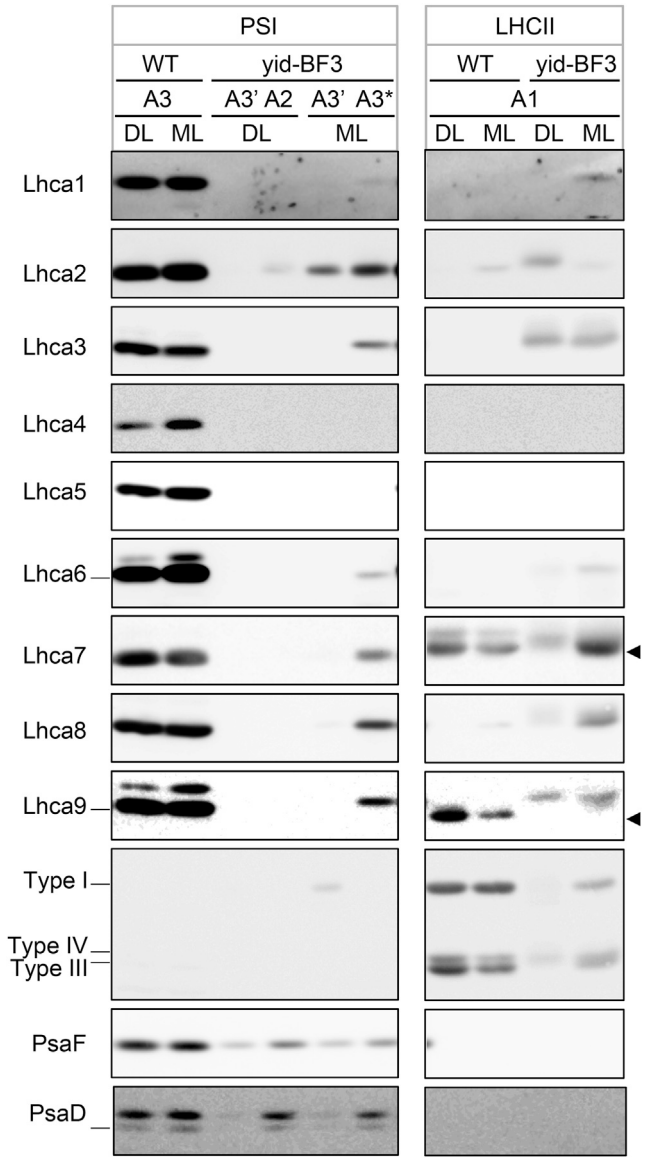

Figure 10. Immunodetection of LHC Subunits in PSI and LHCII Fractions.

PSI fractions (A3) from wild-type (WT) cells grown under DL and ML, A3′, and PSI/PSII fraction (A2) from yid-BF3 grown under DL, and A3′ and PSI fraction (A3*) from yid-BF3 grown under ML, were subjected to immunodetection. The filters were probed with antibodies against LHCI (Lhca1–9) and PSI (PsaD and PsaF), and LHCII that cross-reacts with LHCII types I, III, and IV. Arrowheads indicate cross-reaction with LHCIIs in A1 when probed with anti-Lhca7 and anti-Lhca9 antibodies, respectively. Ten microliters of each fraction were loaded in each lane.

(Laemmli, 1970) for immunochemically detecting PsaA, PsaF, PsaD, PsaL, CP26, CP29, Lhcbm5, and LHCI subunits, a standard system containing 6 M urea in the resolving gel for separating PSII subunits (Takahashi et al., 1996), a system by Schagger and von Jagow (1987) for separation of PsaG, PsaH, PsaK, and PsaN, and a system containing high Tris in the resolving gel by Fling and Gregerson (1986) for detection of LHCI subunits by staining. The separated polypeptides were stained with a fluorescence dye, Flamingo (Bio-Rad), and visualized using an FLA-7000 fluoro-image analyzer (Fujifilm, Tokyo) or electroblotted onto a nitrocellulose filter. Immunodetection was performed using antibodies against PSI, PSII, and LHC subunits. Specificity of these antibodies was tested in Supplemental Figure 1. Signals were visualized by enhanced chemiluminescence (ECL) using a LAS-4000 mini-luminescent image analyzer and were quantified using Multigauge version 3.0 software (Fujifilm, Tokyo). Signals were detected with the increment exposure mode that enables a series of signals to be exposed consecutively, and the data for each signal are added to accumulate exposure data to obtain weak signals or avoid overexposure.

Chlorophyll Content

Chlorophyll concentrations were determined following extraction of the pigments in methanol, as described previously (Porra et al., 1989). For pigment analyses, chlorophylls and carotenoids were extracted from cells in *N*,*N*-dimethylformamide (DMF), applied to an ODS C18 BEH column (2.1 mm × 150 mm) (Waters) at 30°C, and separated using high-performance liquid chromatography (ACUITY, UPLC/PDA system, Waters) as described previously (Ozawa et al., 2012).

Fluorescence Measurements

Fluorescence induction kinetics were performed at room temperature using a DeepGreen Fluorometer (JBeamBio) and a home-built fluorescence CCD camera recorder (Johnson et al., 2009). Maximum efficiency of PSII, F_V/F_M ($F_V = F_M - F_0$), was determined using dark-adapted cells. Maximum fluorescence (F_M) was measured either after a brief and saturating flash of light or during continuous illumination in the presence of 10 μM 3-(3,4-dichlorophenyl)-1, 1-dimethylurea (DCMU). Fluorescence emission spectra (77 K) were measured with a setup built in-house. Samples were immersed in liquid nitrogen and excited with an LED source (LS-450, Ocean Optics; blue LED, 450 nm). The emission spectra were recorded using a CCD spectrophotometer (QE6500, Ocean Optics).

Spectroscopic Studies

Cells were harvested during exponential growth (2×10^6 cells ml^{-1}) and were resuspended at a concentration of 1×10^7 cells ml^{-1} in minimum medium with the addition of 10% (w/v) Ficoll to prevent cell sedimentation during the measurements. The cell suspension was then vigorously stirred in a 50-ml Erlenmeyer flask for 20 min in the dark at 340 rpm.

When absorption changes were measured with a JTS-10 (Bio-Logic, Grenoble, France), the detecting and continuous lights were provided by LEDs and the saturating flash by a dye laser (640 nm) pumped by a second harmonic of a neodymium-doped yttrium aluminum garnet (Nd:YAG) laser (Minilite II, Continuum). The detection wavelength was selected using a 520-nm interferential filter, 10 nm full width at half maximum. PSI and PSII charge separation capacity were calculated from changes in the amplitude of the fast phase (100 μs) of the ECS signal (at 520 nm) upon excitation with a saturating laser flash in the presence or absence of the PSII inhibitors, DCMU (20 μM) and hydroxylamine (1 mM). Light-saturation curves were determined by using absorptive neutral density filters to reduce flash intensity.

When absorption changes were measured with a home-built pump-probe spectrophotometer that allows measurements to be performed in scattering biological material (Béal et al., 1999), the sample was excited at 700 nm, with a 7-ns pulse (full width at half maximum) of varying intensity, obtained by pumping a dye laser (LDS 698) with a frequency-doubled Nd:YAG laser (Brilliant; Quantell). The P700 oxidation level or P700 charge separation yield measured by the 430–445 nm and 520 nm absorbance changes were respectively probed 500 ns and 100 μs after the actinic pulse by 5-ns pulses (full width at half maximum) obtained by pumping an Optical Parametric Oscillator (Panther OPO; Continuum) by a frequency-tripled Nd:YAG laser (Continuum, Surelite) as described previously (Joliot and Joliot, 1999; Byrdin et al., 2006). Absorbance changes were averaged 10 times for each intensity of the excitation (pump) flash, the energy of which was assessed with a laser power and energy meter (Gentec-E).

SUPPLEMENTAL INFORMATION

Supplemental Information is available at *Molecular Plant Online*.

FUNDING

This work was supported by basic funding from CNRS and Université Pierre & Marie Curie Paris 06, by the Agence Nationale de la Recherche contract ANR FtsH-Thyl-Chlamy (ANR-12-BSV8-0011), by the "Initiative d'Excellence" program from the French State (Grant 'DYNAMO', ANR-11-LABX-0011-01), and by the Japan Science and Technology Agency (JST), CREST and JSPS KAKENHI grant numbers 15K14551 and 16H06554. The visit of R.S. in Okayama University was supported by the DST-JSPS India-Japan Cooperative Science Program (13039221-000325).

AUTHOR CONTRIBUTIONS

F.-A.W. and Y.T. devised the project; S.B. performed genetics experiments; S.B., F.R., and F.-A.W. performed biophysics experiments; C.d.V. contributed FtsH experiments; N.K., R.S., and Y.T. performed biochemical experiments; S.B., F.-A.W., and Y.T. wrote the manuscript.

ACKNOWLEDGMENTS

We thank Benjamin Bailleul for advice in the processing of spectroscopic data. No conflict of interest declared.

Received: May 30, 2016
Revised: September 1, 2016
Accepted: October 4, 2016
Published: October 11, 2016

REFERENCES

Allen, K.D., and Staehelin, L.A. (1994). Polypeptide composition, assembly and phosphorylation patterns of the photosystem II antenna system of *Chlamydomonas reinhardtii*. Planta **194**:42–54.

Anderson, J.M. (1986). Photoregulation of the composition, function, and structure of thylakoid membranes. Annu. Rev. Plant Physiol. **37**:93–136.

Bassi, R., Croce, R., Cugini, D., and Sandonà, D. (1999). Mutational analysis of a higher plant antenna protein provides identification of chromophores bound into multiple sites. Proc. Natl. Acad. Sci. USA **96**:10056–10061.

Béal, D., Rappaport, F., and Joliot, P. (1999). A new high-sensitivity 10-ns time-resolution spectrophotometric technique adapted to in vivo analysis of the photosynthetic apparatus. Rev. Sci. Instrum. **70**:202–207.

Byrdin, M., Santabarbara, S., Gu, F., Fairclough, W.V., Heathcote, P., Redding, K., and Rappaport, F. (2006). Assignment of a kinetic component to electron transfer between iron–sulfur clusters FX and FA/B of Photosystem I. Biochim. Biophys. Acta **1757**:1529–1538.

Cahoon, A.B., and Timko, M.P. (2000). yellow-in-the-dark mutants of chlamydomonas lack the CHLL subunit of light-independent protochlorophyllide reductase. Plant Cell **12**:559–569.

Chua, N.H., and Bennoun, P. (1975). Thylakoid membrane polypeptides of *Chlamydomonas reinhardtii*: wild-type and mutant strains deficient in photosystem II reaction center. Proc. Natl. Acad. Sci. USA **72**:2175–2179.

Dall'Osto, L., Bressan, M., and Bassi, R. (2015). Biogenesis of light harvesting proteins. Biochim. Biophys. Acta **1847**:861–871.

de Vitry, C., and Wollman, F.-A. (1988). Changes in phosphorylation of thylakoid membrane proteins in light-harvesting complex mutants from *Chlamydomonas reinhardtii*. Biochim. Biophys. Acta **933**:444–449.

Drop, B., Webber-Birungi, M., Fusetti, F., Kouril, R., Redding, K.E., Boekema, E.J., and Croce, R. (2011). Photosystem I of *Chlamydomonas reinhardtii* contains nine light-harvesting complexes (Lhca) located on one side of the core. J. Biol. Chem. **286**:44878–44887.

Elrad, D., Niyogi, K.K., and Grossman, A.R. (2002). A major light-harvesting polypeptide of photosystem ii functions in thermal dissipation. Plant Cell **14**:1801–1816.

Espineda, C.E., Linford, A.S., Devine, D., and Brusslan, J.A. (1999). The *AtCAO* gene, encoding chlorophyll *a* oxygenase, is required for chlorophyll *b* synthesis in *Arabidopsis thaliana*. Proc. Natl. Acad. Sci. USA **96**:10507–10511.

Ferrante, P., Ballottari, M., Bonente, G., Giuliano, G., and Bassi, R. (2012). LHCBM1 and LHCBM2/7 polypeptides, components of major LHCII complex, have distinct functional roles in photosynthetic antenna system of *Chlamydomonas reinhardtii*. J. Biol. Chem. **287**:16276–16288.

Fling, S.P., and Gregerson, D.S. (1986). Peptide and protein molecular weight determination by electrophoresis using a high-molarity tris buffer system without urea. Anal. Biochem. **155**:83–88.

Ford, C., and Wang, W.-Y. (1980a). Temperature-sensitive yellow mutants of *Chlamydomonas reinhardtii*. Mol. Gen. Genet. **180**:5–10.

Ford, C., and Wang, W.-Y. (1980b). Three new yellow loci in *Chlamydomonas reinhardtii*. Mol. Gen. Genet. **179**:259–263.

Fristedt, R., Willig, A., Granath, P., Crèvecoeur, M., Rochaix, J.-D., and Vener, A.V. (2009). Phosphorylation of photosystem II controls functional macroscopic folding of photosynthetic membranes in *Arabidopsis*. Plant Cell **21**:3950–3964.

Guergova-Kuras, M., Boudreaux, B., Joliot, A., Joliot, P., and Redding, K. (2001). Evidence for two active branches for electron transfer in photosystem I. Proc. Natl. Acad. Sci. USA **98**:4437–4442.

Harris, E.H. (2009). The Chlamydomonas Sourcebook: Introduction to Chlamydomonas and Its Laboratory Use (San Diego, CA: Academic Press).

Hudock, G.A., and Levine, R.P. (1964). Regulation of photosynthesis in *Chlamydomonas reinhardtii*. Plant Physiol. **39**:889–897.

Johnson, X., Vandystadt, G., Bujaldon, S., Wollman, F.-A., Dubois, R., Roussel, P., Alric, J., and Béal, D. (2009). A new setup for in vivo fluorescence imaging of photosynthetic activity. Photosynth. Res. **102**:85–93.

Joliot, P., and Joliot, A. (1999). In vivo analysis of the electron transfer within photosystem I: are the two phylloquinones involved? Biochemistry **38**:11130–11136.

Laemmli, U.K. (1970). Cleavage of structural proteins during the assembly of the head of bacteriophage T4. Nature **227**:680–685.

Liu, Z., Yan, H., Wang, K., Kuang, T., Zhang, J., Gui, L., An, X., and Chang, W. (2004). Crystal structure of spinach major light-harvesting complex at 2.72 A resolution. Nature **428**:287–292.

Malnoë, A., Wang, F., Girard-Bascou, J., Wollman, F.-A., and de Vitry, C. (2014). Thylakoid FtsH protease contributes to photosystem II and cytochrome b_6f remodeling in *Chlamydomonas reinhardtii* under stress conditions. Plant Cell **26**:373–390.

Markwell, J.P., Webber, A.N., and Lake, B. (1985). Mutants of Sweetclover (*Melilotus alba*) lacking Chlorophyll *b*—studies on pigment-protein complexes and thylakoid protein phosphorylation. Plant Physiol. **77**:948–951.

Mazor, Y., Borovikova, A., and Nelson, N. (2015). The structure of plant photosystem I super-complex at 2.8 A resolution. Elife **4**:e07433.

Michel, H., Tellenbach, M., and Boschetti, A. (1983). A chlorophyll *b*-less mutant of *Chlamydomonas reinhardtii* lacking in the light-harvesting chlorophyll *a*/*b*-protein complex but not in its apoproteins. Biochim. Biophys. Acta **725**:417–424.

Minagawa, J., and Takahashi, Y. (2004). Structure, function and assembly of Photosystem II and its light-harvesting proteins. Photosynth. Res. **82**:241–263.

Murray, D.L., and Kohorn, B.D. (1991). Chloroplasts of *Arabidopsis thaliana* homozygous for the ch-1 locus lack chlorophyll *b*, lack stable LHCPII and have stacked thylakoids. Plant Mol. Biol. **16**:71–79.

Natali, A., Roy, L.M., and Croce, R. (2014). In vitro reconstitution of light-harvesting complexes of plants and green algae. J. Vis. Exp., e51852.

Naumann, B., Stauber, E.J., Busch, A., Sommer, F., and Hippler, M. (2005). N-terminal processing of Lhca3 Is a key step in remodeling of the photosystem I-light-harvesting complex under iron deficiency in *Chlamydomonas reinhardtii*. J. Biol. Chem. **280**:20431–20441.

Nawrocki, W.J., Santabarbara, S., Mosebach, L., Wollman, F.-A., and Rappaport, F. (2016). State transitions redistribute rather than dissipate energy between the two photosystems in *Chlamydomonas*. Nat. Plants **2**:16031.

Nick, S., Meurer, J., Soll, J., and Ankele, E. (2013). Nucleus-encoded light-harvesting chlorophyll *a/b* proteins are imported normally into chlorophyll *b*-free chloroplasts of *Arabidopsis*. Mol. Plant **6**:860–871.

Ozawa, S., Onishi, T., and Takahashi, Y. (2010). Identification and characterization of an assembly intermediate subcomplex of photosystem I in the green alga *Chlamydomonas reinhardtii*. J. Biol. Chem. **285**:20072–20079.

Ozawa, S.-i., Kosugi, M., Kashino, Y., Sugimura, T., and Takahashi, Y. (2012). 5′-Monohydroxyphylloquinone is the dominant naphthoquinone of PSI in the green alga *Chlamydomonas reinhardtii*. Plant Cell Physiol. **53**:237–243.

Pan, X., Li, M., Wan, T., Wang, L., Jia, C., Hou, Z., Zhao, X., Zhang, J., and Chang, W. (2011). Structural insights into energy regulation of light-harvesting complex CP29 from spinach. Nat. Struct. Mol. Biol. **18**:309–315.

Peng, L., Fukao, Y., Fujiwara, M., Takami, T., and Shikanai, T. (2009). Efficient operation of NAD(P)H dehydrogenase requires supercomplex formation with photosystem I via minor LHCI in Arabidopsis. Plant Cell **21**:3623–3640.

Picaud, A., and Dubertret, G. (1986). Pigment protein complexes and functional properties of tetratype resulting from crosses between CP_1 and CP_2 less *Chlamydomonas* mutants. Photosynth. Res. **7**:221–236.

Polle, J.E.W., Benemann, J.R., Tanaka, A., and Melis, A. (2000). Photosynthetic apparatus organization and function in the wild type and a chlorophyll *b*-less mutant of *Chlamydomonas reinhardtii*. Dependence on carbon source. Planta **211**:335–344.

Porra, R., Thompson, W., and Kriedemann, P. (1989). Determination of accurate extinction coefficients and simultaneous equations for assaying chlorophylls *a* and *b* extracted with four different solvents: verification of the concentration of chlorophyll standards by atomic absorption spectroscopy. Biochim. Biophys. Acta **975**:384–394.

Qin, X., Suga, M., Kuang, T., and Shen, J.R. (2015). Photosynthesis. Structural basis for energy transfer pathways in the plant PSI-LHCI supercomplex. Science **348**:989–995.

Sager, R. (1955). Inheritance in the green alga *Chlamydomonas reinhardtii*. Genetics **40**:476–489.

Schagger, H., and von Jagow, G. (1987). Tricine-sodium dodecyl sulfate-polyacrylamide gel electrophoresis for the separation of proteins in the range from 1 to 100 kDa. Anal. Biochem. **166**:368–379.

Schmidt, S., Reich, R., and Witt, H.T. (1971). Electrochromism of chlorophylls and carotenoids in multilayers and in chloroplasts. Naturwissenschaften **58**:414.

Schuhmann, H., and Adamska, I. (2012). Deg proteases and their role in protein quality control and processing in different subcellular compartments of the plant cell. Physiol. Plant. **145**:224–234.

Sugimoto, I., and Takahashi, Y. (2003). Evidence that the PsbK polypeptide is associated with the photosystem II core antenna complex CP43. J. Biol. Chem. **278**:45004–45010.

Takabayashi, A., Kurihara, K., Kuwano, M., Kasahara, Y., Tanaka, R., and Tanaka, A. (2011). The Oligomeric states of the photosystems and the light-harvesting complexes in the Chl *b*-less mutant. Plant Cell Physiol. **52**:2103–2114.

Takahashi, Y., Goldschmidt-Clermont, M., Soen, S.Y., Franzen, L.G., and Rochaix, J.D. (1991). Directed chloroplast transformation in *Chlamydomonas reinhardtii*: insertional inactivation of the *psaC* gene encoding the iron sulfur protein destabilizes photosystem I. EMBO J. **10**:2033–2040.

Takahashi, Y., Utsumi, K., Yamamoto, Y., Hatano, A., and Satoh, K. (1996). Genetic engineering of the processing site of D1 precursor protein of photosystem II reaction center in *Chlamydomonas reinhardtii*. Plant Cell Physiol. **37**:161–168.

Takahashi, Y., Yasui, T.A., Stauber, E.J., and Hippler, M. (2004). Comparison of the subunit compositions of the PSI-LHCI supercomplex and the LHCI in the green alga *Chlamydomonas reinhardtii*. Biochemistry **43**:7816–7823.

Takahashi, H., Iwai, M., Takahashi, Y., and Minagawa, J. (2006). Identification of the mobile light-harvesting complex II polypeptides for state transitions in *Chlamydomonas reinhardtii*. Proc. Natl. Acad. Sci. USA **103**:477–482.

Tanaka, A., Ito, H., Tanaka, R., Tanaka, N.K., Yoshida, K., and Okada, K. (1998). Chlorophyll *a* oxygenase (*CAO*) is involved in chlorophyll *b* formation from chlorophyll *a*. Proc. Natl. Acad. Sci. USA **95**:12719–12723.

Terao, T., Yamashita, A., and Katoh, S. (1985). Chlorophyll *b*-deficient mutants of rice II. Antenna chlorophyll *a/b*-proteins of photosystem I and photosystem II. Plant Cell Physiol. **26**:1369–1377.

Wei, L., Derrien, B., Gautier, A., Houille-Vernes, L., Boulouis, A., Saint-Marcoux, D., Malnoe, A., Rappaport, F., de Vitry, C., Vallon, O., et al. (2014). Nitric oxide-triggered remodeling of chloroplast bioenergetics and thylakoid proteins upon nitrogen starvation in *Chlamydomonas reinhardtii*. Plant Cell **26**:353–372.

Witt, H.T. (1979). Energy conversion in the functional membrane of photosynthesis. Analysis by light pulse and electric pulse methods. Biochim. Biophys. Acta **505**:355–427.

Wollman, F.-A., and Bennoun, P. (1982). A new chlorophyll-protein complex related to Photosystem I in *Chlamydomonas reinhardtii*. Biochim. Biophys. Acta **680**:352–360.

Wollman, F.-A., and Delepelaire, P. (1984). Correlation between changes in light energy distribution and changes in thylakoid membrane polypeptide phosphorylation in *Chlamydomonas reinhardtii*. J. Cell Biol. **98**:1–7.

Yoshioka-Nishimura, M., and Yamamoto, Y. (2014). Quality control of Photosystem II: the molecular basis for the action of FtsH protease and the dynamics of the thylakoid membranes. J. Photochem. Photobiol. B Biol. **137**:100–106.

On The Cover Image shows an overlay of bright field and red fluorescence images of a mixture of wild-type and chlorophyll *b*-less mutant cells of *Chlamydomonas reinhardtii*. Significant diminishment of the overall chlorophyll accumulation in the mutant strain results in a loss of two thirds of its fluorescence emission. Image by: Sandrine Bujaldon.